Energy 122 (2017) 748–766

Contents lists available at ScienceDirect

Energy

journal homepage: www.elsevier.com/locate/energy

Gradient decent based multi-objective cultural differential evolution for short-term hydrothermal optimal scheduling of economic emission with integrating wind power and photovoltaic power

Huifeng Zhang [a], Dong Yue [a, *], Xiangpeng Xie [a], Chunxia Dou [a], Feng Sun [b]

[a] Institute of Advanced Technology, The Jiangsu Engineering Laboratory of Big Data Analysis and Control, Nanjing University of Posts and Telecommunications, Nanjing, 210023, China
[b] Guodian Nanjing Automation CO., LTD, Nanjing, 210023, China

ARTICLE INFO

Article history:
Received 16 July 2016
Received in revised form
5 January 2017
Accepted 16 January 2017
Available online 23 January 2017

Keywords:
Gradient decent
Multi-objective optimization
Differential evolution
Economic emission
Optimal scheduling

ABSTRACT

With the integration of wind power and photovoltaic power, optimal operation of hydrothermal power system becomes great challenge due to its non-convex, stochastic and complex-coupled constrained characteristics. This paper extends short-term hydrothermal system optimal model into short-term hydrothermal optimal scheduling of economic emission while considering integrated intermittent energy resources (SHOSEE-IIER). For properly solving SHOSEE-IIER problem, a gradient decent based multi-objective cultural differential evolution (GD-MOCDE) is proposed to improve the optimal efficiency of SHOSEE-IIER combined with three designed knowledge structures, which mainly enhances search ability of differential evolution in the shortest way. With considering those complex-coupled and stochastic constraints, a heuristic constraint-handling measurement is utilized to tackle with them both in coarse and fine tuning way, and probability constraint-handling procedures are taken to properly handle those stochastic constraints combined with their probability density functions. Ultimately, those approaches are implemented on five test systems, which testify the optimization efficiency of proposed GD-MOCDE and constraint-handling efficiency for system load balance, water balance and stochastic constraint-handling measurements, those obtained results reveal that the proposed GD-MOCDE can properly solve the SHOSEE-IIER problem combined with those constraint-handling approaches.

1. Introduction

Short-term hydrothermal optimal scheduling (SHOS) plays an important role in power system operation, it assigns output of hydro plants and thermal units to minimize economic cost subjected to various nonlinear and non-convex constraints over a certain period [1]. Since the source of hydro plants is natural water resource, the main target is to utilize hydro power to reduce the economic cost caused by thermal units. As the importance of SHOS is well recognized, some optimization methods have been proposed to solve this problem, such as genetic evolution [2–5], simulated annealing (SA) [6], evolutionary programming (EP) [7], artificial neural network (ANN) [8], particle swarm optimization (PSO) [9,10], differential evolution (DE) [11] and hybrid evolutionary method [12]. These approaches can tackle with SHOS problem without considering the convexity or differentiability that mathematical methods often require, and have certain ability for searching global optima with relative low computational complexity [13].

Recently, more and more concerns have been taken on environmental pollution, which has great influence on society life quality. The major emission pollution caused by thermal power plant is NO_x produced by the burning coal, it generally has two choices to prevent emission pollutant [14]. One choice is to replace those old equipment with cleaner ones, which needs to pay expensive price for replacing, it can be only taken as a long-term option. The emission dispatch option is an effective short-term alternative as the other choice, which needs to optimize both economic cost and emission pollutant. Since economic cost and emission pollutant can be considered as two paradoxical problems, short-term hydrothermal optimal scheduling with economic emission (SHOSEE) problem becomes a multi-objective

* Corresponding author.
E-mail address: medongy@vip.163.com (D. Yue).

http://dx.doi.org/10.1016/j.energy.2017.01.083
0360-5442/

optimization problem (MOP) with fuel cost and emission volume to be minimized [15]. Generally, there are two main research directions: weighted method and optimize those objectives simultaneously. The first direction is mainly to convert multiple objectives into single objective problem (SOP) with trade-off weights, then many methods can be used to optimize the single objective problem. The second direction is to optimize these objectives simultaneously with Pareto dominance order, and produce a set of non-dominated solutions in single simulation run. Though the trade-off method can obtain the optimal scheme, it may lead to two disadvantages: (1) It can produce only one solution after each simulation run, once trade-off weights are changed, the whole optimization must be set up again; (2) It is difficult to yield true Pareto front especially when objective functions are non-convex or consisted of disconnected Pareto fronts [16]. Therefore, Pareto optimization strategy is utilized to solve optimal scheduling problem by optimizing emission rate and economic cost simultaneously in this paper. Recent studies demonstrate that population based evolutionary algorithms performs well for solving MOPs due to its independence of problem representation and optimization efficiency for solving SOP. The most popular methods of those multi-objective evolutionary algorithms (MOEAs) are Deb's NSGA-II [17], Zitzler's SPEA2 [18], MOPSO [19,20] and MODE [21–23]. These approaches can obtain a set of non-dominated solutions in single simulation run, but it may either suffer from premature convergence problem at different degrees or have relative low search ability.

With the increasing renewable energy resources integrated into power system operation, it brings about great challenge for optimal scheduling of hybrid energy system due to its stochastic characteristics, and more researchers become to focus on this research interest. Literature [24] takes wind power into consideration in SHOSEE problem, and produces a set of non-dominated solutions with NSGA-II method. Literature [25] presents an optimization model for short-term hydrothermal scheduling that performs a co-optimization of energy and reserves for tertiary regulation with considering hydrology uncertainty and forced outages of generation units and transmission lines. Literature [26] utilizes a novel nature inspired optimization algorithm named ant lion optimization for solving wind integrated hydrothermal power generation scheduling problem, and implements this algorithm on four standard test systems and its efficiency is verified by its obtained simulation results. Though the above methods in reported literature can tackle with these optimal scheduling problems, they can't optimize the emission volume and fuel cost simultaneously.

In comparison to those reported literature, this paper extends hydrothermal system into hybrid energy system with integrating wind power and photovoltaic power, which brings great difficulty for solving optimal scheduling of hydro-thermal-wind-photovoltaic power system. Gradient decent based multi-objective cultural differential evolution is proposed for solving optimal scheduling of hybrid energy resource system with integrating wind power and photovoltaic power in this paper. Gradient decent based mutation operator is proposed to improve the search ability of differential evolution with its adaptive parameters, which can guide the search process on the shortest way. In order to handle the randomness of wind power and photovoltaic power, the random constraint limits are converted into the deterministic interval information combining with considering its probability density function. Furthermore, the proposed gradient decent based multi-objective cultural differential evolution algorithm is carried on the hybrid energy resource system, and the obtained results verify the feasibility and efficiency of the proposed GD-MOCDE.

The construction of this paper is presented as follows: The problem formulation is introduced in Section 2, the principle of multi-objective cultural differential evolution is presented in Section 3, gradient decent based multi-objective cultural differential evolution and constraint-handling approaches are proposed in Section 4, and its implementation and case study are presented in Section 5 and Section 6.

2. Problem formulation

The hybrid energy resource system mainly consists of hydropower, thermal power, wind power and photovoltaic power. The target of SHOSEE-IIER is to minimize the fuel cost and emission volume caused by thermal units, which requires proper assignment of power output by each power generator to decrease thermal output while considering water balance constraint, system load balance constraint and various basic constraint limits of each power generator.

2.1. The objective of economic cost

The fuel cost of hybrid energy resources is caused by thermal power, traditional formulation of fuel cost objective can't reflects the sharp increase of fuel cost in reality, it can be described as the objective of classical ED with considering valve point effects, it consists of fuel cost in N_c generating units for T time intervals, which can be presented as follows [27]:

$$\min F_1 = \sum_{t=1}^{T}\sum_{i=1}^{N_c}\left[a_i + b_i P_{cit} + c_i P_{cit}^2 + \left|d_i \sin\left(e_i\left(P_{ci,\min} - P_{cit}\right)\right)\right|\right] \tag{1}$$

Where F_1 denotes fuel cost objective of thermal power system, P_{cit} is the generated power in the i-th thermal unit at t-th time interval, T is the length of total dispatch period, N_c is the number of thermal units, a_i, b_i, c_i, d_i, e_i are the coefficients of the i-th thermal unit, $P_{ci,\min}$ is the minimum output of the i-th thermal unit.

2.2. The objective of emission rate

With the increasing concern on the emission pollutant of thermal units, more and more focuses are taken on the emission rate of harmful gases. The nitric oxide can be taken as the representative harmful gas caused by thermal units [27], and the total emission rate of thermal power system can be presented as follows [17]:

$$\min F_2 = \sum_{t=1}^{T}\sum_{i=1}^{N_c}\left[\alpha_i + \beta_i P_{cit} + \gamma_i P_{cit}^2 + \zeta_i \exp(\lambda_i P_{cit})\right] \tag{2}$$

Where F_2 denotes emission rate of thermal power system, and $\alpha_i, \beta_i, \gamma_i, \zeta_i, \lambda_i$ are the coefficients of emission rate at the i-th thermal unit.

2.3. Constraints

Since wind power and photovoltaic power are incorporated into hydro-thermal power system, stochastic characteristics of intermittent energy resources must be considered in the optimal scheduling while satisfying output limits of each power generator, ramp rate limits, water volume balance and system load balance constraints.

(1) System load balance constraint [28]:

$$\sum_{l=1}^{N_h} P_{hlt} + \sum_{i=1}^{N_c} P_{cit} + \sum_{j=1}^{N_w} P_{wjt} + \sum_{k=1}^{N_p} P_{pkt} = P_{Dt} + P_{Lt} \tag{3}$$

Where P_{hlt} is output of the l-th hydro plant at t-th time interval, P_{wjt} is the output of the j-th wind farm at t-th time interval, P_{pkt} is the output of the k-th photovoltaic field at t-th time interval, N_h, N_w and N_p are the number of hydro plants, wind farms and photovoltaic fields, P_{Dt} denotes the system load at t-th time period, P_{Lt} is the transmission loss at t-th time period, it is merely related to thermal output, and it can be expressed as follows:

$$P_{Lt} = \sum_{i=1}^{N_c} \sum_{j=1}^{N_c} P_{cit} B_{ij} P_{cjt} + \sum_{i=1}^{N_c} B_{0i} P_{cit} + B_{00} \tag{4}$$

WhereB_{ij}, B_{0i} and B_{00} are loss coefficients at the i-th thermal unit.

(2) Power generation limits:

$$\begin{cases} P_{ci,\min} \le P_{cit} \le P_{ci,\max}, i = 1,2,...,N_c, t = 1,2,...,T. \\ \Pr ob\left(P_{wj,\min} \le P_{wjt} \le P_{wj,\max}\right) = \rho_w, j = 1,2,...,N_w, t = 1,2,...,T. \\ \Pr ob\left(P_{pk,\min} \le P_{pkt} \le P_{pk,\max}\right) = \rho_p, k = 1,2,...,N_p, t = 1,2,...,T. \end{cases} \tag{5}$$

Where $P_{ci,\min}, P_{ci,\max}$ are the minimum and maximum outputs of the i-th thermal unit, $P_{wj,\min}, P_{wj,\max}$ are the minimum and maximum outputs of the j-th wind farm, $P_{pk,\min}, P_{pk,\max}$ are the minimum and maximum outputs of the k-th photovoltaic field.

(3) Generating unit ramp rate limits:

$$\begin{cases} DR_{ci} \le P_{cit} - P_{ci,t-1} \le UR_{ci}, \ \ i = 1,2,...,N_c, t = 1,2,...,T. \\ DR_{wj} \le P_{wjt} - P_{wj,t-1} \le UR_{wj}, \ \ j = 1,2,...,N_w, t = 1,2,...,T. \\ DR_{pk} \le P_{pkt} - P_{pk,t-1} \le UR_{pk}, \ \ k = 1,2,...,N_p, t = 1,2,...,T. \end{cases} \tag{6}$$

Where UR_{ci}, DR_{ci} are the up-ramp and down-ramp limits of the i-th thermal unit, UR_{wj}, DR_{wj} are the up-ramp and down-ramp limits of the j-th wind farm, UR_{pk}, DR_{pk} are the up-ramp and down-ramp limits of the k-th photovoltaic field.

(4) The constraint limits of hydropower plant:

Generally, hydro power output can be expressed with quadratic function of reservoir water head and water discharge, and water head can be also expressed with reservoir storage. Therefore, hydro power output can be in terms of reservoir storage and water discharge, which can be formulated as follows:

$$P_{hlt} = C_{1l}{*}V_{hlt}^2 + C_{2l}{*}Q_{hlt}^2 + C_{3l}{*}V_{hlt}{*}Q_{hlt} + C_{4l}{*}V_{hlt} + C_{5l}{*}Q_{hlt} + C_{6l} \tag{7}$$

Where $C_{1l}, C_{2l}, C_{3l}, C_{4l}, C_{5l}, C_{6l}$ are the coefficients of the l-th hydro plant, V_{hlt} is the reservoir storage of the l-th hydro plant at t-th time interval, Q_{hlt} is the water discharge of the l-th hydro plant at t-th time interval.

Simultaneously, topology of those hydro plants can also have great effect on the optimal scheduling of hydropower system, and water balance among water discharge, reservoir storage and water inflow should satisfy the following formulation:

$$V_{hlt} = V_{hl,t-1} + \left[I_{lt} - Q_{hlt} - S_{lt} + \sum_{k=1}^{N_l}\left(Q_{hl,t-\tau_l^k} + S_{l,t-\tau_l^k}\right)\right]\Delta t$$
$$l = 1,2,...,N_h; t = 1,2,...,T; 0 \le \tau_l^k \le T \tag{8}$$

Where I_{lt} is inflow water at the l-th hydro plant at t-th time interval, S_{lt} is water spillage of the l-th hydro plant at t-th time period, τ_l^k is the transmission delay between the l-th hydro plant and the k-th upstream hydro plant at l-th hydro plant.

For properly scheduling the hydro power generation in next day, initial storage and terminal storage of hydro plant are known as follows:

$$V_{hl0} = V_{l,begin}, V_{hlT} = V_{l,end} \quad (i = 1,2,...,N_h) \tag{9}$$

Where $V_{l,begin}$ is the initial reservoir storage at l-th hydro plant, and $V_{l,end}$ is the terminal storage at l-th hydro plant.

3. The multi-objective cultural differential evolution (MOCDE)

Based on the multi-objective differential evolution, culture algorithm can provide culture knowledge structures for population space evolution, several knowledge structures can provide elite experience, normative information and historical information, which can guide multi-objective differential evolution of population space to the global optimal solution.

3.1. The principles of differential evolution

DE has been widely utilized due to its simple but powerful search ability in real-world application. It mainly consists of three evolution operators: mutation, crossover and selection, mutation and crossover operators are applied on the individual to yield trial vector, and selection operator determines whether the trial vector needs to be added into the population of next generation [29]. The mutation operator of DE/rand/1/bin strategy can be demonstrated as follows:

$$V_{r,G+1} = X_{r,G} + F{*}\left[\left(X_{r1,G} - X_{r2,G}\right) + \left(X_{r3,G} - X_{r4,G}\right)\right], \quad r1 \ne r2 \ne r3 \ne r4 \ne r \tag{10}$$

Where $X_{r1,G}, X_{r2,G}, X_{r3,G}, X_{r4,G}$ are selected from non-dominated population, $r1, r2, r3, r4 \in \{1,2,...,NP\}$ are the integer index of the non-dominated population, NP is the size of non-dominated population, $V_{r,G+1}$ is the parameter vector for $G+1$-th generation, F is the mutation parameter, it is range in $[0,2]$. The detail of crossover operator and selection operator can be seen in literature [29].

3.2. The culture knowledge structure for multi-objective differential evolution

The culture algorithm (CA) was proposed by Reynolds [30], it consists of belief space, population space and communication protocols, population space connects to belief space by those communications. The population space produce the offspring individual by Generate() function, and evaluate the fitness of individuals with Objective() function, and optimal individuals are selected by Select() function. The belief space accepts the experience of optimal individuals by Accept() function, elite experience of belief space is updated by update() function, and these elite experience can guide the population evolution in the population space.

The framework of culture algorithm is presented in Fig. 1.

Belief space has various knowledge structures, situational knowledge, normative knowledge and historical knowledge structures have been proposed by Saleem [31]. The evolutionary algorithm can be integrated into the knowledge structure, and the efficiency of culture algorithm mainly depends on the knowledge structures. In this paper, the situational knowledge, normative knowledge and historical knowledge structures are redesigned for multi-objective differential evolution for dynamic economic emission dispatch.

4. The gradient decent based multi-objective cultural differential evolution for dynamic economic emission dispatch of hybrid energy resource system

In order to solve dynamic economic emission dispatch problem of hybrid energy resource system properly, some improvements have been proposed on the multi-objective culture differential evolution. The gradient decent based mutation operator is proposed to accelerate the search ability of differential evolution, which takes the shortest path to the optimal solution with gradient decent method [32–34]. Furthermore, several knowledge structures are redefined according to the problem formulation of dynamic economic emission dispatch of hybrid energy resource system, which can provide convenience for population space evolution. Due to those complex-coupled constraint in hybrid energy resource system, stochastic constraints of wind power and photovoltaic power are converted into deterministic constraints, and system load balance constraint is properly handled by a two-step coupled constraint-handling technique.

4.1. Gradient decent based mutation operator

It is known that the decent gradient represents the fastest direction of objective increasing or decreasing, which can provide fast search direction during the differential evolution. This paper proposes a decent gradient based mutation operator, which improves the search ability of differential evolution [35].

For a given multi-objective function $f(x) = [f_1(x), f_2(x), ..., f_m(x)]^T, x \in R^n$, the gradient of function $f(x)$ can be defined in terms of Jacobian matrix as follows:

$$\nabla_{m\times n} f(x) = \begin{bmatrix} \frac{\partial f_1(x)}{\partial x_1} & \frac{\partial f_2(x)}{\partial x_2} & \cdots & \frac{\partial f_1(x)}{\partial x_n} \\ \frac{\partial f_2(x)}{\partial x_1} & \frac{\partial f_2(x)}{\partial x_2} & \cdots & \frac{\partial f_2(x)}{\partial x_n} \\ \vdots & \vdots & \vdots & \vdots \\ \frac{\partial f_m(x)}{\partial x_1} & \frac{\partial f_m(x)}{\partial x_2} & \cdots & \frac{\partial f_m(x)}{\partial x_n} \end{bmatrix} = \begin{bmatrix} (\nabla f_1)^T \\ (\nabla f_2)^T \\ \vdots \\ (\nabla f_m)^T \end{bmatrix} \tag{11}$$

The ∇f_i represents the gradient direction, and $\frac{\partial f_i}{\partial x_j}$ $(i = 1, 2...m, j = 1, 2...n)$ is the partial derivative. For a given positive space H^+ and negative space H^-, the element $y \in R^n$ in these two spaces satisfy following conditions:

$$\begin{cases} H^+ = \left\{ y \in R^n \middle| \nabla f(x)^T y > 0 \right\} \\ H^- = \left\{ y \in R^n \middle| \nabla f(x)^T y < 0 \right\} \end{cases} \tag{12}$$

The positive direction leads the decision vector $y \in R^n$ to the direction that objective function decreases, and the negative directive leads it to the opposite direction. For the iterative vector $X_{G+1}, X_G (X_{G+1}$ is near to $X_G)$, the negative gradient needs to satisfy [35]:

$$F_i(X_{G+1}) - F_i(X_G) = \nabla F_i(X_{G+1} - X_G) < 0 \tag{13}$$

The above formulation describes the path that X_G moves to X_{G+1} on the i th objective direction. For simplicity, two objective optimization problem is taken for example, gradient direction of Pareto front changes as it is shown in Fig. 2. The optimal Pareto front in G-th generation converts to the Pareto front in the G+1-th generation on the gradient direction, it can be seen that the gradient direction of multi-objective optimization can be represented by the weighted

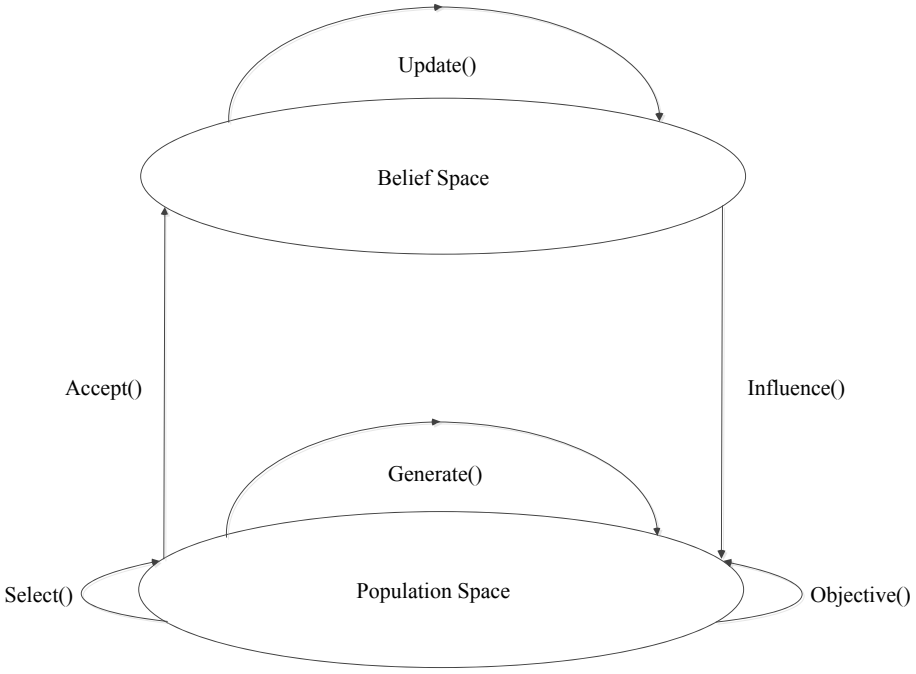

Fig. 1. The Framework of culture algorithm.

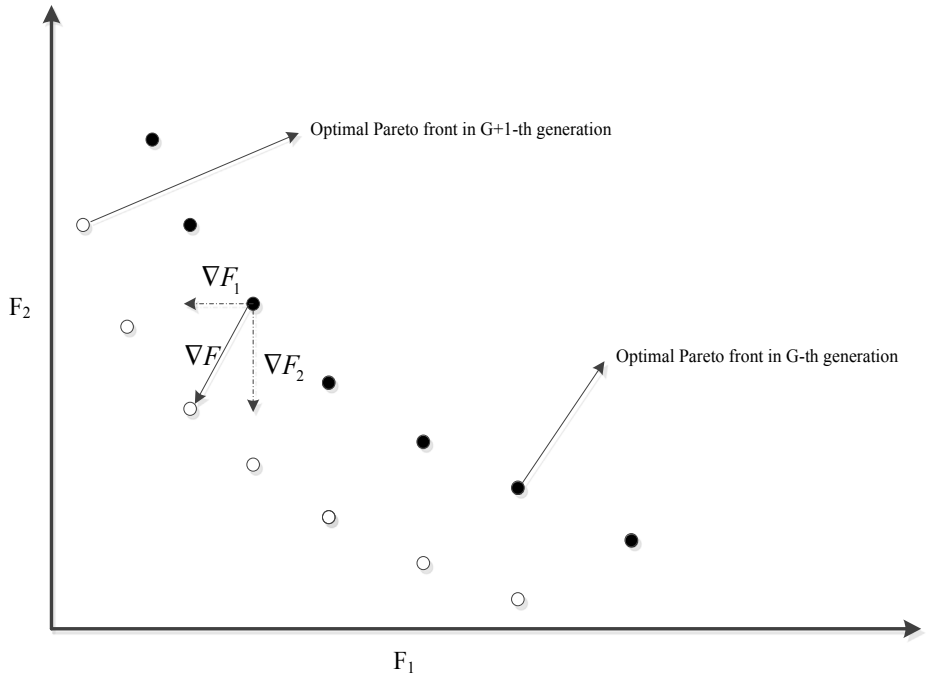

Fig. 2. The gradient direction of Pareto front during the evolution process.

sum of gradient direction on each objective.

According to the results obtained in literature [35], the vector in the negative space can be taken:

$$y = -\sum_{i=1}^{m} \lambda_i \frac{\nabla f_i(x)}{\|\nabla f_i(x)\|} \tag{14}$$

Where λ_i is weighted parameter in interval $[0, 1]$, $\|\cdot\|$ represents the Euclidian norm. The vector can ensure $\nabla F y < 0$, hence $y \in H^-$. The iterative vector in Formula (12) satisfy the following condition:

$$\nabla F(X_{G+1} - X_G) = \nabla F y \tag{15}$$

Then the derivation $X_{G+1} - X_G$ can be equally described as:

$$X_{G+1} - X_G = \eta_G y = -\eta_G \sum_{i=1}^{m} \lambda_i \frac{\nabla f_i(x)}{\|\nabla f_i(x)\|} \tag{16}$$

Where $\eta_G \in R^+$ represents scaling parameter. Since ∇f_i can't be obtained since the objective in formulation (1) is non-differentiable. To avoid the derivative on the objective, the gradient of two objective on the j th dimension of decision variable can be replaced in discrete way by following formulation:

$$\nabla f_i(x_j) = \frac{f_i(x_j + \Delta x_j) - f_i(x_j)}{\Delta x_j} \tag{17}$$

Where

$$X_{G+1}^j = X_G^j + \gamma_1^j (X_{r_2,G} - X_{r_3,G}) + \gamma_2^j (X_{r_4,G} - X_{r_5,G}) \tag{18}$$

Where the parameters are set as follows:

$$\gamma_1^j = \frac{-\eta_G \lambda_1 \cdot \mathrm{sgn}(f_1(X_{r_2,G}) - f_1(X_{r_3,G}))}{\left(X_{r_2,G}^j - X_{r_3,G}^j\right)^2 \sqrt{\sum_{j=1}^{n} \frac{1}{\left(X_{r_2,G}^j - X_{r_3,G}^j\right)^2}}}$$

$$\gamma_2^j = \frac{-\eta_G \lambda_2 \cdot \mathrm{sgn}(f_2(X_{r_4,G}) - f_2(X_{r_5,G}))}{\left(X_{r_4,G}^j - X_{r_5,G}^j\right)^2 \sqrt{\sum_{j=1}^{n} \frac{1}{\left(X_{r_4,G}^j - X_{r_5,G}^j\right)^2}}} \tag{19}$$

$$\eta_G = \eta_0 [(g_{\max} - G + 1)/g_{\max}]^p$$

According to the above obtained differential evolution, the search ability can be enhanced for seeking the shortest way to the optimal solution, the search direction can be obtained by summation of weighted two directions, which depend on the search direction of two objectives. Hence, this gradient decent method is proposed to improve the mutation operator for increasing the search ability of differential evolution.

4.2. Knowledge structure designed for gradient decent based multi-objective differential evolution

Due to high efficiency for dealing with single objective optimization problem, CA has been extended to solve multi-objective optimization problem. In this paper, gradient decent based multi-objective differential evolution is embedded into the computational model provided by CA, and local random search (LRS) is also integrated into the historical knowledge structure of CA, which can avoid the premature problem caused by gradient decent based differential evolution at certain degree. In the population space, constraint limits of all those decision variables are stored in the normative knowledge structure, which can be interpreted as legal restraints in human society. Ultimately, the obtained elite experience during population space evolution is stored in the situational knowledge structure, which can guide the population space

evolution.

4.2.1. Historical knowledge structure

Generally, historical knowledge is mainly utilized to find the patterns especially when the environment changes, and used to solve dynamic functions [36]. Due to great ability of gradient decent based differential evolution, it may tend to fall into the local optima, which suffers the premature problem as other evolutionary algorithm does. Here, LRS operation is used to overcome the premature problem by increasing the population diversity and exploit the promising area to get global optima.

The LRS presented in literature [37] improves the performance of DE for properly solving DED problem, DE is utilized to seek the available optimal area that global optima may be within, LRS operator is mainly used obtain the global optima from these local optimal solutions. The implementation of LRS can be generally taken as follows:

Step 1: Initialization. Combining with the differential evolution process, current optimal individual X_G is taken as initial individual X_{opt}, and set iteration step m as 0.

Step 2: Search scale setting. For a given real number $\theta \in (0,1]$, the initial search scale S_0 can be defined as follows:

$$S_0 = \theta * (X_{\max} - X_{\min}) \tag{20}$$

Where $X_{\max}, X_{\min}$ are the maximum and minimum individual, and search scale needs to change adaptively for searching the global optima:

$$S_m = (1-\rho) * S_{m-1} \tag{21}$$

Where ρ is the scaling parameter in the interval $[0,1)$.

Step 3: Local optima generating. In order to avoid falling into the local optima, N_l local optimal individuals need to be generated as follows:

$$X_m^n = X_{opt} + R_m * rnd(D,1), \quad n = 1,2,...,N_l \tag{22}$$

Where $rnd(D,1)$ is the D-dimensional uniform random number in the interval $[-1,1]$, if the value of local optimal individual violates the constraint limits, the constraint handling mechanism is taken to force it into the feasible area.

Step 4: Global optima selection. Dominance relationship can be obtained between the current optimal individual X_{opt} and those generated individuals. If $X_m^n \succ X_{opt}$ (X_m^n dominates X_{opt}), then set $X_{opt} = X_m^n$.

Step 5: Termination criterion. If $m < L_{\max}$ ($L_{\max}$ is the maximum iteration number), then $m = m + 1$ and go to **Step 2**, otherwise, the LRS process is terminated, and the obtained X_{opt} can be taken as the optimal individual of LRS operation.

4.2.2. Normative knowledge structure

Due to those varieties of constraint limits in the hybrid energy resource system, those constraint limit information needs to be stored for convenience. The redefined normative knowledge structure mainly stores the interval information in hybrid energy resource system, and the constraints in problem formulation need to be converted into the interval formation. For properly controlling the constraint violation problem during the constraint handing process and population space evolution, all those variables that violates the constraint limits can be forced into the feasible domain. Generally, the following measurement can be taken:

$$x_i' = \begin{cases} l_i & if \ \ x_i < l_i \\ x_i & if \ \ l_i \le x_i \le u_i \\ u_i & if \ \ x_i \ge u_i \end{cases} \tag{23}$$

Where l_i, u_i are the upper and lower bound, x_i represents the i−th dimensional value of decision variable. Furthermore, ramp rate constraint can be converted into interval information combing with the output constraint limits, the output limit of each power generator can be presented as follows:

$$\begin{cases} \max(P_{ci,t-1} + DR_{ci}, \ P_{ci,\min}) \le P_{cit} \le \min(P_{ci,t-1} + UR_{ci}, \ P_{ci,\max}) \\ \max(P_{wj,t-1} + DR_{wj}, \ P_{wj,\min}) \le P_{wjt} \le \min(P_{wj,t-1} + UR_{wj}, \ P_{wj,\max}) \\ \max\left(P_{pk,t-1} + DR_{pk}, \ P_{pk,\min}\right) \le P_{pkt} \le \min\left(P_{pk,t-1} + UR_{pk}, \ P_{pk,\max}\right) \end{cases} \tag{24}$$

Where $P_{wj,\min}$, $P_{wj,\max}$, $P_{pk,\min}$, $P_{pk,\max}$ are the obtained low and upper bound after transforming stochastic constraint into deterministic constraint.

4.2.3. Situational knowledge structure

The situational knowledge structure mainly takes charge of storing the elite experience obtained in the population space evolution, and this elite experience can guide the population evolution by influence () protocol in return. The archive retention mechanism can be integrated into this knowledge structure, and the elite experience of non-dominated individual is stored. For a newly obtained individual, whether it can be added into the archive set needs to satisfy following norms:

(1) If the newly generated individual can dominate one individual in the archive set, delete all those individuals dominated by it, and add the new individual into the archive set and its elite experience is stored in the situational knowledge structure.
(2) If the newly generated individual can be dominated by the individual in the archive set, it can't be added into the archive set.
(3) If the newly generated individual can't dominate any individual in the archive set and also can't be dominated by any individual in the archive set, check the diversity distribution of Pareto front before it is added and after it is added, which can be found in literature [22]. If it has better diversity distribution after the newly generated individual is added, it can be added into the archive set and its elite experience can be stored in the situational knowledge structure. Otherwise, it can't be added into the archive set.

4.3. Constraint handling for solving dynamic economic emission dispatch problem of multiple energy resource system

Since intermittent energy resources have been jointed into the energy system, more complex constraints and great randomness can be taken into the optimal dispatch of hybrid energy resource

system. In comparison to those traditional energy resources, the output limits of intermittent energy resources are uncertain, which brings great challenges to the dynamic economic emission dispatch of multiple energy resource system.

4.3.1. Constraint handling for probability constraint limits of photovoltaic power output

Since the output process of wind power and photovoltaic power has strong randomness, output limits can be only demonstrated with probability terms as it is shown in Formula (5). However, it is difficult to deal with the probability constraint in the optimization process, it needs to convert the probability constraint into the deterministic constraint first. Here, the probability constraint can be properly handled as follows:

Firstly, the value of wind output needs to be normalized with $\eta_j = x_{pj}/x_{pj\max}$, it assumes that η_j follows the Beta distribution [38,39], and its probability density function is described as:

$$f\left(\eta_j\right) = \frac{1}{B(\alpha,\beta)}\eta_j^{\alpha-1}\left(1-\eta_j\right)^{\beta-1},\quad 0 \le \eta_j \le 1 \tag{25}$$

Then its distribution function can be obtained:

$$F(\xi_j) = \frac{\int_0^{\xi_j} \varpi_j^{\alpha-1}(1-\varpi_j)^{\beta-1}d\varpi_j}{B(\alpha,\beta)},\quad 0<\xi_j<1 \tag{26}$$

It equals 0 when $\xi_j < 0$, and equals 1 when $\xi_j \ge 1$. The $B(\cdot)$ represents the beta function with its two parameters α, β. Then probability constraint of output limits can be converted as [39]:

$$x_{pj\max} * F^{-1}(1-\rho) \le x_{pj} \le x_{pj\max} * F^{-1}(\rho) \tag{27}$$

4.3.2. Constraint handling for probability constraint limits of wind power output

It is known that wind power generation is closely related to the wind speed, the relationship between wind power output and wind speed can be described as:

$$P_{wj} = \begin{cases} 0, & v_j < v_{j,in} \ \ or \ \ v_j \ge v_{j,out} \\ P_{wj,\max} * \dfrac{v_j - v_{j,in}}{v_{j,rate} - v_{j,in}}, & v_{j,in} \le v_j < v_{j,rate} \\ P_{wj,\max}, & v_{j,rate} \le v_j < v_{j,out} \end{cases} \tag{28}$$

where $P_{wj,\max}, v_{j,rate}$ are the rated output (or maximum output) and rated wind speed at the j th wind turbine, $v_{j,in}, v_{j,out}$ are the cut-in and cut-out wind speed at the j th wind turbine. The wind output can not be zero when wind speed is between cut-in speed and cut-out speed, it has direct ratio relation with wind speed when wind speed is between cut-in speed and rated wind speed, and it works at the maximum output especially when wind speed ranges in the rated wind speed and cut-out speed. In literature [40], the probability density function and cumulative distribution function of wind speed can be described as follows:

$$\begin{cases} f(v_j) = (k/c)(v_j/c)^{k-1}\exp\left(-(v_j/c)^k\right), & v_j \ge 0 \\ F_w(v_j) = 1 - \exp\left(-(v_j/c)^k\right), & v_j \ge 0 \end{cases} \tag{29}$$

where k, c are the scaling parameters. According to the relationship presented in Formula (29), the cumulative distribution function of wind power output can be obtained as:

$$\begin{aligned} F_w(P_{wj}) = 1 - \exp\left\{-\left[\left(1 + \frac{v_{j,rate} - v_{j,in}}{v_{j,in}\mathrm{P}_{wj\max}}P_{wj}\right)\frac{v_{j,in}}{c}\right]^k\right\} \\ + \exp\left[-(v_{j,out}/c)^k\right],\quad 0 \le P_{wj} < \mathrm{P}_{wj\max} \end{aligned} \tag{30}$$

Combining with the method presented in Section 4.3.1, the deterministic interval can be obtained as:

$$F_w^{-1}(1-\rho) \le x_{wit} \le F_w^{-1}(\rho) \tag{31}$$

4.3.3. Constraint handling technique for water volume balance

If cascaded hydro power is taken into consideration, water volume balance can be a headache during optimization process especially in hybrid energy operation system. Generally, it must be tackled properly before handling system load balance since other energy resource can't affect the hydro power output. Here, heuristic constraint handling method is taken to deal with water volume balance, it mainly controls the feasible domain by coarse adjustment and fine tuning technique, which can be presented in detail in literature [11].

4.3.4. Initial priority optimization strategy on constraint handling for system load balance

Constraint handling efficiency has great influence on the optimization results especially when the hybrid energy resource system has series of complex-coupled constraints, the two-step constraint handling technique is used to tackle with this problem. Besides, since fuel cost and emission pollutant are mainly produced by thermal units, wind power and photovoltaic power need to be make full use to decrease the thermal output, which can produce operation scheme near to the optimal scheme and reduce the computational complexity of the whole population evolution. In this paper, wind power and photovoltaic power are given relative high priority level at the initial step of each time period, the initial priority optimization strategy is presented before the constraint handling process [41].

Step 1: For simplicity, the output of thermal power, wind power and photovoltaic power is noted as $P_{\theta,t}$ (it represents thermal power when $1 \le \theta \le N_c$, wind power when $N_c + 1 \le \theta \le N_c + N_w$, and photovoltaic power when $N_c + N_w \le \theta \le N_c + N_w + N_p$), and set $t = 1$, go to **Step 2**.

Step 2: Initialize the output of thermal power, wind power and photovoltaic power, and wind power and photovoltaic power is given priority as follows:

$$\begin{cases} P_{\theta,t} = P'_{c\theta,\min} + rand(0,1) * \left[P'_{c\theta,\max} - P'_{c\theta,\min}\right], & \theta = 1,2,\ldots,N_c \\ P_{\theta,t} = P'_{w,\theta-N_c,\min} + 0.9 * \left[P'_{w,\theta-N_c,\max} - P'_{w,\theta-N_c,\min}\right], & \theta = N_c+1, N_c+2,\ldots,N_c+N_w \\ P_{\theta,t} = P'_{p,\theta-N_c-N_w,\min} + 0.9 * \left[P'_{p,\theta-N_c-N_w,\max} - P'_{p,\theta-N_c-N_w,\min}\right], & \theta = N_c+N_w+1, N_c+N_w+2,\ldots,N_c+N_w+N_p \end{cases} \tag{32}$$

Where $rand(0,1)$ is random number in interval $(0,1]$, $P'_{c\theta,\min}, P'_{c\theta,\max}$, $P'_{w,\theta-N_c,\min}, P'_{w,\theta-N_c,\max}$ and $P'_{p,\theta-N_c-N_w,\min}$, $P'_{p,\theta-N_c-N_w,\max}$ are the obtained minimum and maximum output of thermal power, wind power and photovoltaic power, which can be obtained in normative knowledge in Section 4.2.2, and go to **Step 3**.

Step 3: Calculate the output deviation with Formula (32) If $\Delta P_t < \varepsilon_p$ (ε_p represents the permitted output accuracy), it represents that the system load balance is properly handled, and go to **Step 8**; Otherwise, a coupled coarse tuning method is implemented to tackle with it.

$$\Delta P_t = P_{D,t} + P_{loss,t} - \sum_{\theta=1}^{N_c+N_w+N_p} P_{\theta,t} \tag{33}$$

Set coarse iteration number $I_{coa} = 0$, and let all the power generator bears the output violation equally, and modify their output with Formula (33) and go to **Step 4**:

$$\begin{cases} \Delta P_{ave,t} = \Delta P_t / (N_c + N_w + N_p) \\ P_{\theta,t} = P_{\theta,t} + \Delta P_{ave,t} \end{cases} \tag{34}$$

Step 4: If the modified output exceeds the constraint limits, the measurements in the normative knowledge can force the output into the feasible domain. Set the iteration number of fine tuning $I_{fine} = 0$ and then go to **Step 5**.

Step 5: Calculate the output deviation with Formula (32) again. If $\Delta P_t < \varepsilon_p$ is satisfied, go to Step. Otherwise, choose a random unit number r, and modify the power output with Formula (34), go to **Step 6**.

$$P_{r,t} = P_{r,t} + \Delta P_{ave,t} \tag{35}$$

Step 6: If the modified output exceeds the constraint limits, force it to the feasible domain with Formula (22). If $I_{fine} < I_{fine,\max}$($I_{fine,\max}$ is the maximum iteration number of fine tuning), $I_{fine} = I_{fine} + 1$, and go to **Step 5**. Otherwise, go to **Step 7**.

Step 7: If $I_{coa} < I_{coa,\max}$($I_{coa,\max}$ is the maximum iteration number of coarse adjusting), then $I_{coa} = I_{coa} + 1$ and go to **Step 3**. Otherwise, go to **Step 8**.

Step 8: If $t < T$, $t = t + 1$ and go to **Step 2**. Otherwise, system load balance constraint of each time period is properly handled after above procedures, and the constraint handling strategy is terminated.

4.3.5. Feasible selection mechanism for constraint handling technique

Since dynamic economic emission dispatch of hybrid energy resource system consists of several constraint limits of photovoltaic power, wind power and thermal power, the constraint handling technique for these constraint limits plays an important role in the efficiency of dynamic economic emission dispatch of hybrid energy resource system. According to methods in above sections, these limits can be controlled in certain degree, but the modified individual still can be an infeasible one due to its finite iterations, it needs to ensure the feasible characteristics of the modified individual. Here, the total violation can be defined as:

$$Totalviolate\ (X_i) = \sum_{t=1}^{T} |\Delta P_t(X_i)| + \sum_{t=1}^{T} |\Delta W_{water,t}| \tag{36}$$

Where the deviation $\Delta P_t(X_i) = \sum_{i=1}^{N_w} P_{wit} + \sum_{j=1}^{N_p} P_{pjt} + \sum_{k=1}^{N_c} P_{ckt} - L_t$, $\Delta W_{water,t}$ is water balance violation, the modified individual can be taken as a feasible individual if $Totalviolate(X_i) < \varepsilon_p$ (ε_p is the permitted accuracy), and the modified individual can be taken as an infeasible individual if $Totalviolate\ (X_i) \geq \varepsilon_p$. In the selection operator, the feasible individual can be quite important, and generally several norms need to be followed [42]:

(1) If there is one feasible individual and one infeasible individual, select the feasible individual.
(2) If there are two infeasible individuals, select the individual that has less violation.
(3) If there are two feasible individuals, the selection mechanism can be implemented according to the situational knowledge in Section 4.2.3.

5. The implementation of gradient decent based multi-objective cultural differential evolution for solving dynamic economic emission dispatch problem of multiple energy resource system

Since the formulated model contains different power generators, the implementation of the proposed algorithm can be different from optimal dispatch of thermal units. The wind power and photovoltaic power has relative low output capacity and no relationship with fuel cost and emission pollutant, they can be treated priority to thermal power, which can also improve the optimization efficiency. Therefore, priority optimization strategy can be implemented before constraint handling and population evolution. The flowchart of gradient decent based multi-objective cultural differential evolution for solving optimal scheduling of hybrid energy resource system is shown in Fig. 3.

6. Case study

For testifying the efficiency of the proposed gradient decent based multi-objective cultural differential evolution, five test systems are designed in this case study. Test system 1 consists of 10 thermal units with considering transmission loss while integrating no wind power or photovoltaic power in 24 time periods. For testifying the efficiency of priority optimization strategy further, test system 2 is constructed with 30 thermal units with considering transmission loss in 24 time periods. Test system 3 consists of 4 thermal units, 1 wind farm and 1 photovoltaic field with considering the transmission loss between thermal units in 24 time periods. Test system 4 consists of four hydro plants and three thermal units with valve-point effect while considering transmission loss, but ramp rate of each power generator is not taken into consideration. Test system 5 presents a hybrid energy system consisted of four hydro plants, three thermal units, two wind farms and one photovoltaic fields, and all constraint limits are taken into consideration.

6.1. Test system 1: dynamic emission economic dispatch (DEED) with 10 thermal units while considering transmission loss

In this test system, all the data details can be found in literature [17], the output of each thermal unit at each time period is taken as the decision variable, each individual contains the output data of ten thermal units at 24 time periods with an interval of an hour. Here, the proposed GD-MOCDE is implemented on this test system in comparison with MODE, the obtained Pareto front is presented in Fig. 4, it consists of 30 representative non-dominated schemes, which can be seen in Table 1.

In comparison to MODE, the Pareto front obtain by the proposed GD-MOCDE has wide diversity distribution, all the non-dominated schemes are evenly distributed, and the maximum and minimum

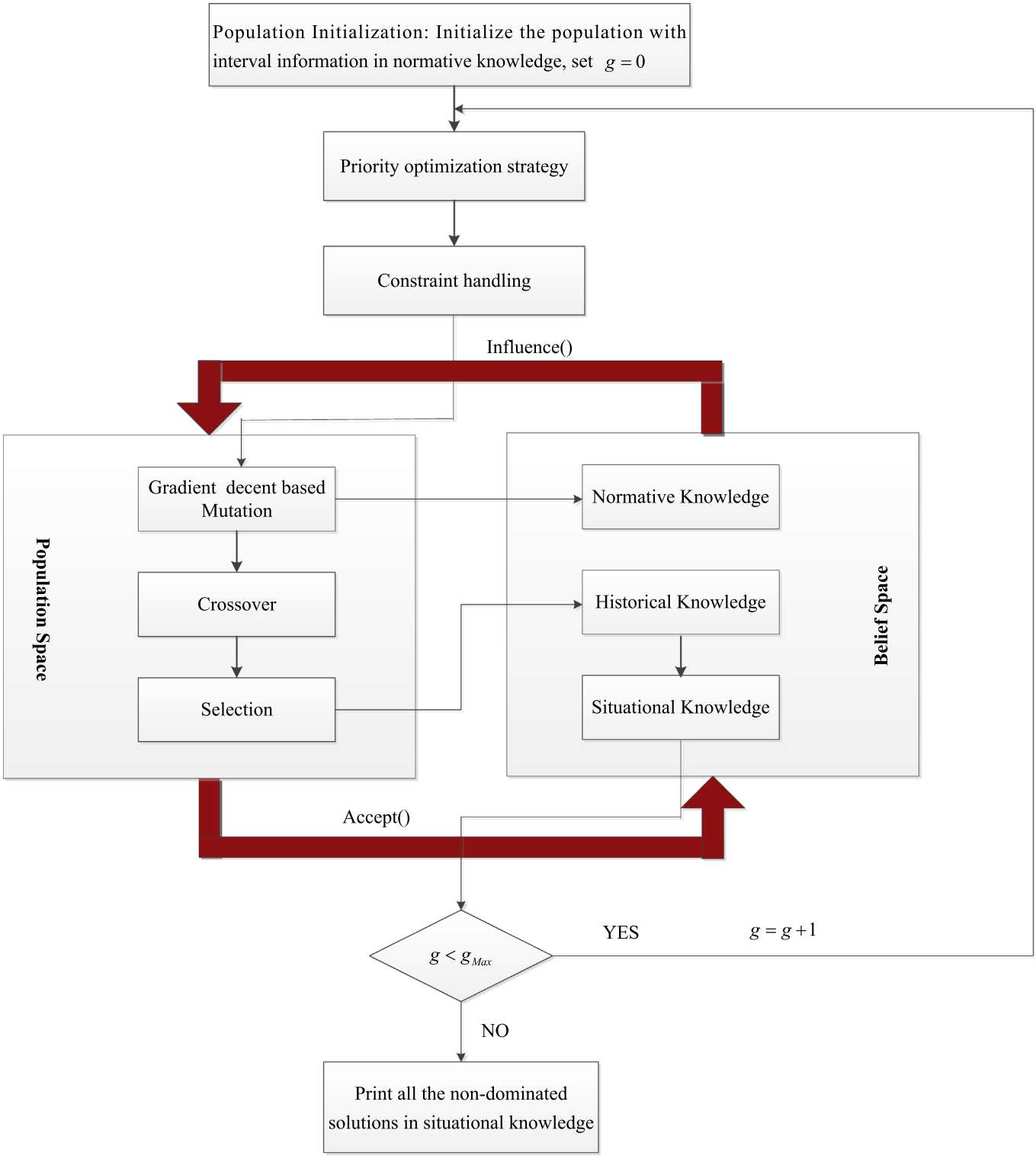

Fig. 3. The flowchart of gradient decent based multi-objective cultural differential evolution for solving optimal scheduling of hybrid energy resource system.

value of economic cost and emission rate are included. Moreover, the obtained non-dominated schemes can dominates that by MODE, which can also be seen in Table 1.

In Table 1, 30 representative non-dominated schemes on Pareto front are presented, the economic cost is range from 2480000 $ to 2559000 $ and emission rate is between 295000 lb and 307000 lb. The obtained minimum economic cost and emission rate by GD-MOCDE is smaller than that of MODE. In comparison to other alternatives, the proposed GD-MOCDE can also have promising results, which can be seen in Table 2.

Since all the non-dominated schemes are evenly distributed, scheme (15) can be taken as the compromise scheme for simplicity. In comparison to other alternatives, scheme (15) by GD-MOCDE has the minimum economic cost and relative small emission rate, and

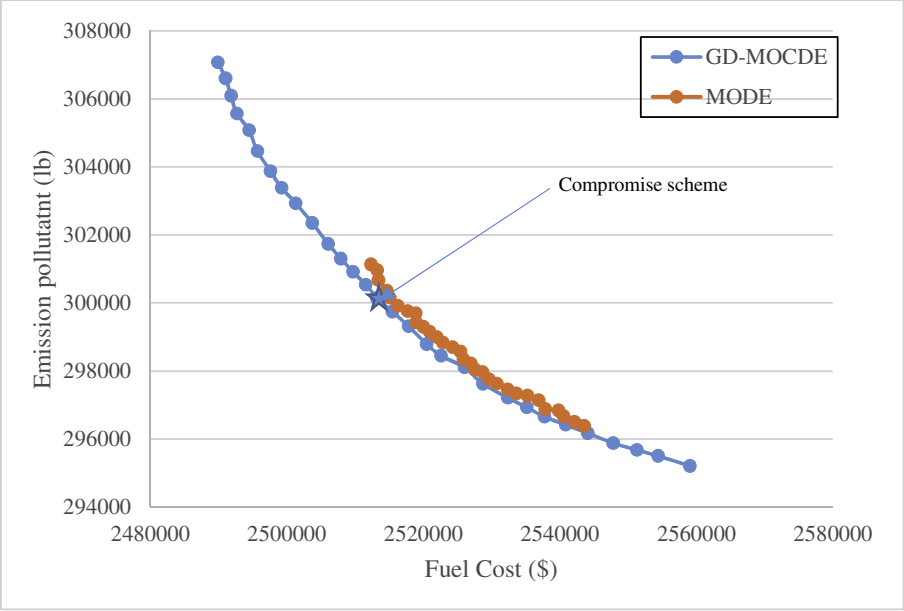

Fig. 4. The comparison of obtained schemes by GD-MOCDE and MODE for test system 1.

Table 1
The obtained non-dominated schemes between GD-MOCDE and MODE for test system 1.

Scheme	GD-MOCDE		MODE		Scheme	GD-MOCDE		MODE	
	Cost($)	Emission (lb)	Cost($)	Emission (lb)		Cost($)	Emission (lb)	Cost($)	Emission (lb)
1	2489890	307080	2512327	301130	16	2515458	299748	2525841	298344
2	2491028	306605	2513241	300963	17	2517832	299319	2526950	298219
3	2491822	306094	2513410	300671	18	2520478	298792	2527591	298046
4	2492678	305567	2514657	300362	19	2522612	298452	2528678	297976
5	2494439	305083	2515118	300156	20	2526021	298105	2529593	297754
6	2495685	304463	2516254	299927	21	2528746	297624	2530748	297634
7	2497590	303877	2517691	299764	22	2532389	297213	2532349	297467
8	2499230	303384	2518886	299698	23	2535183	296931	2533627	297336
9	2501296	302937	2518916	299434	24	2537752	296656	2535237	297278
10	2503713	302353	2520008	299295	25	2540856	296420	2536875	297147
11	2506041	301743	2520942	299161	26	2544095	296175	2537852	296888
12	2507926	301301	2521992	298996	27	2547820	295879	2539795	296844
13	2509660	300924	2522867	298836	28	2551325	295681	2540534	296675
14	2511560	300541	2524285	298703	29	2554396	295502	2542125	296515
15	2513263	300141	2525429	298580	30	2559089	295215	2543560	296387

Table 2
The comparison among optimization alternatives in literature [17,43,44].

Methods	Minimum cost		Minimum emission		Compromise result	
	Cost($)	Emission(lb)	Cost($)	Emission(lb)	Cost($)	Emission(lb)
NSGA-II [17]	–	–	–	–	2522600	309940
RCGA [17]	2516800	317400	265630	304120	2525100	312460
IBFA [43]	2481773	327501	2614341	295883	2517116	299036
MAMODE [44]	2492451	315119	2581621	295244	2514113	302742
MODE	2512327	301130	2543560	296387	2525429	298580
GD-MOCDE	**2489890**	**307080**	**2559089**	**295215**	**2513263**	**300141**

its dispatch process is presented in Table 3, which can be taken for further analysis on the efficiency of the proposed GD-MOCDE. In Table 3, the output of 10 the thermal units at 24 time periods is presented with system load and transmission loss. It can be found that the obtained output of each thermal unit at each time period is controlled in the feasible constraint limits, and the transmission loss is range from 19 MW to 93 MW. Moreover, the transmission loss at each time period can't exceed the 5% of the system load, which also means that system load balance constraint is properly controlled.

According to the analysis on the obtained results, the proposed GD-MOCDE has better performance than that of MODE, which reveals that the gradient decent based mutation operator has more powerful search ability than DE. Furthermore, since culture algorithm is integrated into the differential evolution with three knowledge structures, which provides more convenience for

Table 3
The output (MW) details of compromise scheme obtained by GD-MOCDE for test system 1.

Hours	P_1	P_2	P_3	P_4	P_5	P_6	P_7	P_8	P_9	P_{10}	Load	Loss
1	150	135	78.8	102.64	122.819	122.615	129.441	119.96	79.988	14.381	1036	19.644
2	150	135	80.719	119.347	172.141	122.786	129.539	119.983	80	22.928	1110	22.443
3	150	135.944	134.221	130.638	202.304	160	129.641	120	80	43.769	1258	28.517
4	150	174.864	182.467	180.638	223.275	160	130	119.979	80	40.513	1406	35.736
5	150	214.411	185.026	183.266	242.33	160	130	120	80	55	1480	40.033
6	200.039	219.709	236.219	233.266	242.806	160	129.906	120	80	54.987	1628	48.932
7	222.369	223.316	282.286	241.185	242.951	160	129.969	120	80	53.765	1702	53.841
8	231.064	274.325	283.617	258.289	243	160	130	120	80	55	1776	59.295
9	297.629	310.299	299.235	300	243	159.986	129.995	120	79.995	54.918	1924	71.057
10	335.804	338.087	340	300	243	160	130	120	80	54.68	2022	79.571
11	377.668	388.48	339.829	299.968	243	160	130	120	80	54.946	2106	87.891
12	402.803	411.799	340	300	242.987	160	129.888	120	80	55	2150	92.477
13	361.874	366.699	339.982	299.944	243	159.962	130	120	80	55	2072	84.461
14	300.405	309.374	300.266	299.976	242.893	160	130	120	79.989	52.193	1924	71.096
15	226.506	267.339	291.41	261.998	243	159.934	130	119.989	80	55	1776	59.176
16	164.252	222.342	211.573	233.852	243	160	130	120	80	33.203	1554	44.222
17	152.217	220.91	186.139	183.852	243	160	130	120	80	43.975	1480	40.093
18	225.945	222.472	209.02	231.826	243	160	130	120	80	55	1628	49.263
19	226.92	268.024	279.554	272.688	242.987	160	130	120	80	55	1776	59.173
20	304.747	317.342	337.171	299.768	243	159.974	130	119.989	79.922	55	1972	74.913
21	302.573	302.927	311.8	289.762	243	160	130	120	80	55	1924	71.062
22	222.573	222.927	231.8	239.762	235.796	160	129.595	120	80	34.713	1628	49.166
23	150	143.652	151.8	189.762	211.122	159.955	130	120	79.998	27.55	1332	31.839
24	150	135	105.349	139.762	171.46	158.427	129.534	119.925	80	19.799	1184	25.256

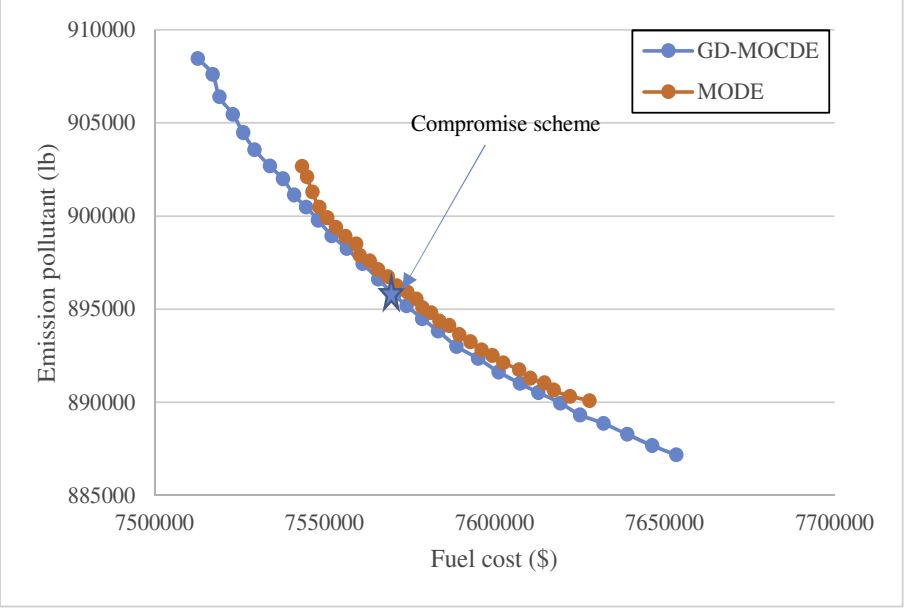

Fig. 5. The comparison of obtained schemes by GD-MOCDE and MODE for test system 2.

population space evolution with constraint handling measurements.

The parameters setting on this test system can be presented as follows: The maximum generation number g_{max} is set to 1000, the size of evolutionary population and archive set are 50 and 30, the initial scaling parameter η_0 is set to 0.8, the permitted output accuracy is set to 0.01, total run time of the proposed GD-MOCDE is 127s with 4.23s to generate each scheme.

6.2. Test system 2: DEED with 30 thermal units while considering transmission loss

On the basis of test system 1, test system 2 extends 10 thermal units to 30 thermal units by tripling the 10 thermal units, all data details can also be found in literature [28]. Here, the proposed GD-MOCDE is implemented on this test system, and the obtained Pareto front is presented in Fig. 5, its representative non-dominated schemes are shown in Table 4.

In Fig. 5, it can be seen that the Pareto front consists of several non-dominated schemes, it has wider diversity distribution than that of MODE [22], which reveals that the maximum and minimum schemes are included in the Pareto front by GD-MOCDE. Moreover, the non-dominated schemes by MODE can be dominated by that of GD-MOCDE, which can be versified according to the data list shown in Table 4. The scheme by GD-MOCDE can dominate the scheme by MODE when their economic cost or emission rate is close to each other.

According to the comparison between GD-MOCDE and MODE,

Table 4
The obtained non-dominated schemes between GD-MOCDE and MODE for test system 2.

Scheme	GD-MOCDE		MODE		Scheme	GD-MOCDE		MODE	
	Cost($)	Emission (lb)	Cost($)	Emission (lb)		Cost($)	Emission (lb)	Cost($)	Emission (lb)
1	7512698	908460	7543339	902682	16	7,570,424	895784	7578806	895074
2	7517057	907615	7544834	902102	17	7574099	895183	7581397	894805
3	7519031	906404	7546358	901297	18	7578714	894493	7583755	894362
4	7523032	905460	7548404	900480	19	7583391	893828	7586708	894118
5	7526022	904477	7550745	899914	20	7588798	893004	7589605	893632
6	7529408	903564	7553308	899391	21	7595174	892349	7592825	893249
7	7533904	902690	7556104	898905	22	7601177	891633	7596125	892823
8	7537738	902009	7559272	898515	23	7607476	891011	7599293	892509
9	7540961	901140	7560360	897886	24	7612856	890525	7602521	892117
10	7544545	900481	7563322	897586	25	7619351	889958	7607167	891745
11	7548101	899782	7565701	897142	26	7625108	889321	7610479	891286
12	7552086	898947	7568593	896755	27	7631962	888874	7614611	891036
13	7556468	898253	7571145	896269	28	7638948	888281	7617423	890654
14	7561210	897445	7574349	895908	29	7646313	887677	7622183	890320
15	7565745	896624	7576973	895544	30	7653408	887176	7627960	890081

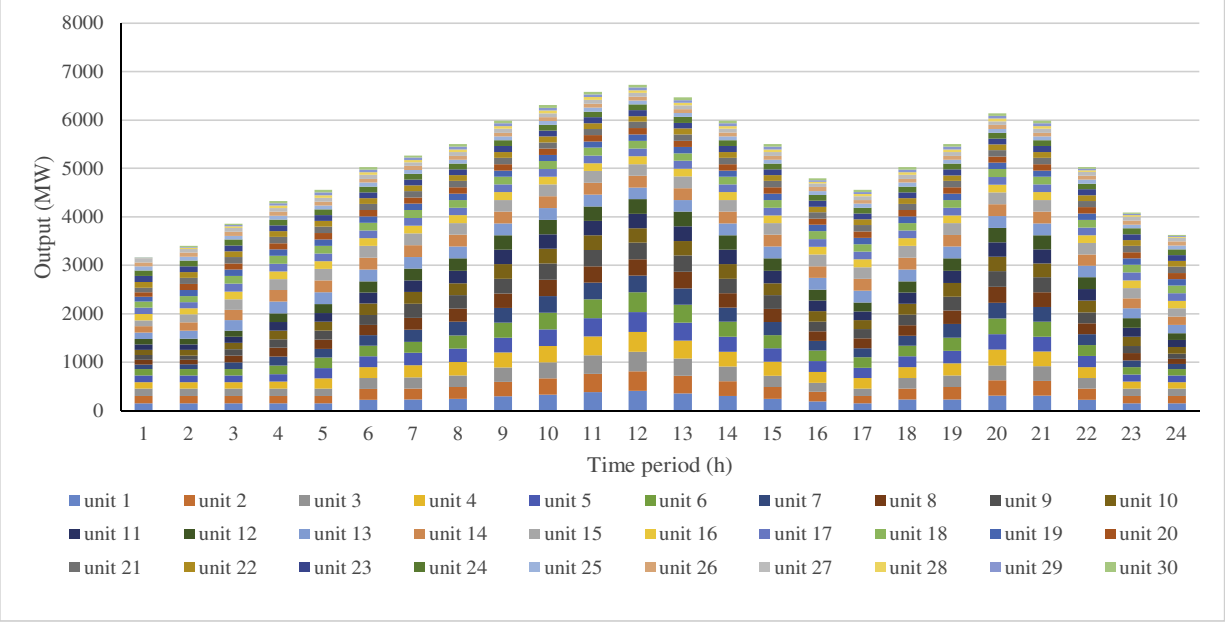

Fig. 6. The output (MW) process of compromise scheme obtained by GD-MOCDE for test system 2.

Table 5
The system load and transmission loss for test system 2.

Hour	1	2	3	4	5	6	7	8	9	10	11	12
Load (MW)	3108	3330	3774	4218	4440	4884	5106	5328	5772	6066	6318	6450
Loss (MW)	58.659	67.196	85.498	106.977	120.067	147.743	162.259	178.341	213.088	238.68	263.677	277.445
Hour	13	14	15	16	17	18	19	20	21	22	23	24
Load (MW)	6216	5772	5328	4662	4440	4884	5328	5916	5772	4884	3996	3552
Loss (MW)	253.331	213.332	178.392	133.499	120.04	147.752	177.779	225.169	213.343	147.645	95.631	75.743

GD-MOCDE has more powerful search ability than MODE due to its efficient gradient decent based mutation operator. For further analysis on the efficiency of the proposed GD-MOCDE on the larger scale of thermal system, scheme (16) is taken as the compromise scheme, which is also labeled in Fig. 5. The output process in scheme (16) is presented in Fig. 6, where the output of 30 thermal units can be seen at each time period.

Each bar represents the output of 30 thermal units at one time period, the bar of different colors presents the cumulative output of different thermal units. Since the transmission loss is taken into consideration, the transmission loss and system load at each time period is shown in Table 5. It can be seen that the transmission loss is range from 50 MW to 280 MW, and actually the obtained transmission loss doesn't exceed 5% of system load at each time period, which also reveals that the constraint handling technique is efficient on this DEED problem.

In this DEED problem of larger-scale thermal system, the proposed GD-MOCDE also has excellent performance and keeps all the

constraint limits under control. According to the comparison and analysis, GD-MOCDE can tackle with complex DEED problem due to its powerful search ability and constraint handling ability, which also reveals that the proposed GD-MOCDE can provide a promising way for complex system with multiple constraints or even stochastic constraints.

The parameter setting is presented as follows: The maximum generation number of GD-MOCDE and MODE is 2000, the size of evolutionary population and archive set are 50 and 30, the initial scaling parameter η_0 is set to 0.9, the permitted output accuracy is set to 0.05, and total run time of the proposed GD-MOCDE is 332s with 11.07s to generate each scheme.

6.3. Test system 3: DEED with 10 power generators with integrating wind power and photovoltaic power while considering transmission loss

The test system 3 consists of 7 thermal units combining with 2 wind farms and 1 photovoltaic field, and the transmission loss is also taken into consideration. In comparison to the DEED in test system 1, thermal unit 8 and thermal unit 9 are replaced by two wind farms, and thermal unit 10 is replaced by photovoltaic field. The wind speed data is adopted in literature [45], which is shown in Table 6. All the optimization parameter settings are the same as that in test system 1, which can be seen in Section 6.1.

According to the wind speed predicted in Table 6, the output P_{rate} is set to 120 MW, wind speed v_{in}, v_{rate} and v_{out} are set as 5 m/s, 15 m/s and 45 m/s, then the possible output of wind farm #1 and wind farm #2 can be calculated by formulation (27), which is presented in Table 7. Since power generation of wind turbine relays more on the wind speed, and the predicted power output can be taken as the maximum output. Here, it is assumed that the wind farm and photovoltaic power can be adjusted, the confidence interval needs to be taken into consideration due to the uncertainty of wind power.

With the probability density and cumulative distribution information presented in Section 4.3.2, the output confidence interval of wind farm #1 and wind farm#2 can be properly obtained. If the degree of confidence ρ that the constraint limits are satisfied in Formula (5) is set to 0.8, the maximum output of wind farm #1 and wind farm #2 can be calculated as 103.4637 MW and 68.97582 MW. The parameter c is set to 15, and k is set to 2.2. Combining with the constraint limits of their output, the confidence interval of wind farm #1 and wind farm #2 are $[47,\ 103.467]$ and $[20,\ 68.976]$.

Simultaneously, power generator is taken as the photovoltaic power generator, its probability density and cumulative distribution functions are presented in Section 4.3.1. According to the constraint handling method presented in Section 4.3.2, the confidence interval of photovoltaic output can be obtained. The parameter α and β are set to 2.0 and 1.0, the degree of confidence is set to 0.8. According to the calculation in Section 4.3.1, the confidence interval of photovoltaic power output is obtained as $[10, 49.194]$.

On the basis of above analysis, the proposed GD-MOCDE is implemented on this test system, the parameter settings are taken as the same as that in test system 1, and the obtained Pareto front is presented in Fig. 7. For testifying the efficiency of the proposed GD-MOCDE, MODE is taken for comparison. It can be seen that the obtained Pareto front by GD-MOCDE is prior to that of MODE on both the convergence ability and diversity distribution, the non-dominated schemes on the Pareto front can dominate that of MODE.

The obtained 30 non-dominated schemes by GD-MOCDE and MODE are shown in Table 8. Since the number of thermal units in test system 3 decreases to 7, it can be seen that the total fuel cost and emission rate decreases in comparison to test system 1. Each obtained scheme by GD-MOCDE can dominate that of MODE on the identical fuel cost or emission rate, which means that the proposed GD-MOCDE has more powerful search ability than that of MODE for solving DEED of hybrid energy resource system.

For further analysis on the dispatching scheme obtained by GD-MOCDE, scheme (15) is taken as the compromise scheme, the output process of thermal units, wind farms and photovoltaic power generator is presented in Fig. 8. The output of different power generators is properly controlled in the feasible domain, and the ramp rate of each power generator is properly satisfied. It can be seen that two wind farms keep the maximum output under the confidence degree $\rho = 0.8$, and photovoltaic power generator also sustains the maximum output at the most time periods, which reveals that the renewable energy resources are made full use. Moreover, the transmission loss of each time period is also controlled under 5% in Table 9, which means that system load balance is properly handled.

According to above analysis on the DEED with several renewable energy resources, DEED problem become random while wind power and photovoltaic power integrating into the thermal power system, but if thermal cost, emission rate and transmission loss are

Table 6
The predicted wind speed on wind farm #1 and wind farm #2 for test system 3.

Hour	1	2	3	4	5	6	7	8	9	10	11	12
Farm1 (m/s)	13.25	14	12.75	11.90	12.50	13.90	11.80	12.75	12.90	12.20	15	13.25
Farm2 (m/s)	11.80	12.00	12.20	12.40	12.50	14.00	15.00	14.50	13.00	13.75	13.40	13.40
Hour	13	14	15	16	17	18	19	20	21	22	23	24
Farm1 (m/s)	14.30	14.10	14.25	11.75	13.75	12.60	11.50	11.90	14.50	16.00	12.70	13.00
Farm2 (m/s)	12.80	12.25	11.40	11.50	11.00	11.25	11.10	11.00	11.45	11.80	11.75	12.25

Table 7
The corresponding output of wind farm #1 and wind farm #2 for test system 3.

Hour	1	2	3	4	5	6	7	8	9	10	11	12
Farm1 (MW)	99	108	93	82.8	90	106.8	81.6	93	94.8	86.4	120	99
Farm2 (MW)	54.4	56	57.6	59.2	60	72	80	76	64	70	67.2	67.2
Hour	13	14	15	16	17	18	19	20	21	22	23	24
Farm1 (MW)	111.6	109.2	111	81	105	91.2	78	82.8	114	120	92.4	96
Farm2 (MW)	62.4	58	51.2	52	48	50	48.8	48	51.6	54.4	54	58

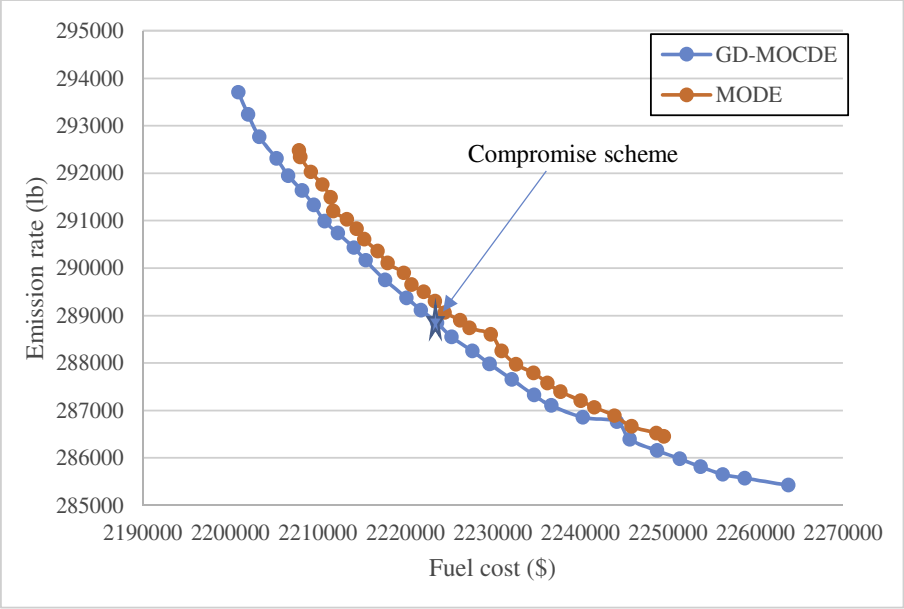

Fig. 7. The comparison of obtained schemes by GD-MOCDE and MODE for test system 3.

Table 8
The obtained non-dominated schemes between GD-MOCDE and MODE for test system 3.

Scheme	GD-MOCDE		MODE		Scheme	GD-MOCDE		MODE	
	Cost($)	Emission (lb)	Cost($)	Emission (lb)		Cost($)	Emission (lb)	Cost($)	Emission (lb)
1	2200904	293703	2207832	292481	16	2225285	288550	2224511	289066
2	2202041	293239	2207989	292342	17	2227651	288253	2226246	288904
3	2203305	292763	2209192	292024	18	2229635	287981	2227331	288742
4	2205260	292314	2210514	291762	19	2232181	287655	2229743	288605
5	2206621	291948	2211452	291491	20	2234701	287323	2231000	288254
6	2208186	291635	2211779	291202	21	2236676	287103	2232643	287971
7	2209525	291331	2213304	291030	22	2240295	286857	2234637	287792
8	2210766	290988	2214425	290824	23	2244159	286764	2236219	287579
9	2212286	290735	2215299	290606	24	2245663	286391	2237735	287397
10	2214109	290431	2216824	290359	25	2248779	286156	2240027	287210
11	2215468	290164	2217965	290104	26	2251362	285983	2241597	287066
12	2217679	289751	2219817	289901	27	2253721	285817	2243899	286893
13	2220142	289374	2220712	289655	28	2256267	285655	2245851	286663
14	2221791	289118	2222088	289498	29	2258783	285577	2248671	286525
15	2223621	288851	2223385	289302	30	2263760	285424	2249552	286454

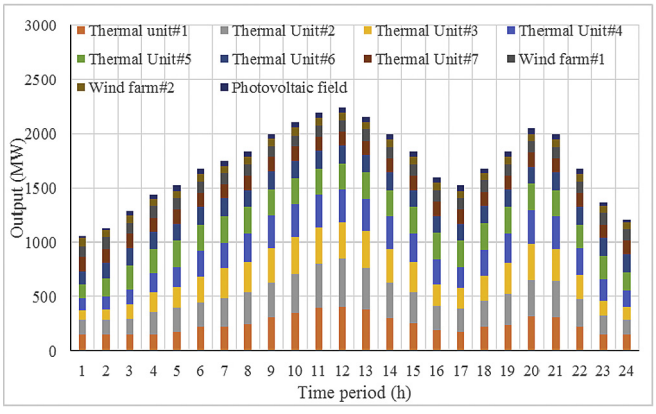

Fig. 8. The output (MW) details of compromise scheme under the degree of confidence $\rho = 0.8$ for test system 3.

taken for the main goal of DEED, these renewable energy resources need to be make full use, which provides a new challenge for solving DEED due to the uncertainty of wind power and photovoltaic power. This paper takes the confidence interval to replace the power generation capacity of wind farm and photovoltaic power, which can be a relative feasible and reliable for solving this problem. Furthermore, the obtained results also reveal that the proposed GD-MOCDE can properly solve this DEED problem with its constraint handling technique for uncertainty in wind power and photovoltaic power.

6.4. Test system 4: hydrothermal optimal scheduling with transmission loss

The hydrothermal system mainly consists of four hydro plants coupled hydraulically and three thermal units, and the topology of four hydro plants (or reservoirs) is shown in Fig. 9. Reservoir 1 and reservoir 2 are located on the upstream of reservoir 3, which is also on the upstream of reservoir 4. The entire scheduling horizon is 24 h with each hour an interval, system load demand, water inflows, output limits and coefficients of hydro plants and thermal units can be seen from literature [7], and comparisons between

Table 9
The transmission loss under the degree of confidence $\rho = 0.8$ test system 3.

Period(h)	1	2	3	4	5	6	7	8	9	10	11	12
Loss (MW)	19.545	22.305	28.511	36.035	40.363	49.322	54.315	59.718	71.506	80.206	88.624	93.241
Period(h)	13	14	15	16	17	18	19	20	21	22	23	24
Loss (MW)	85.156	71.414	59.792	44.586	40.295	49.391	59.542	75.452	71.678	49.677	32.12	25.166

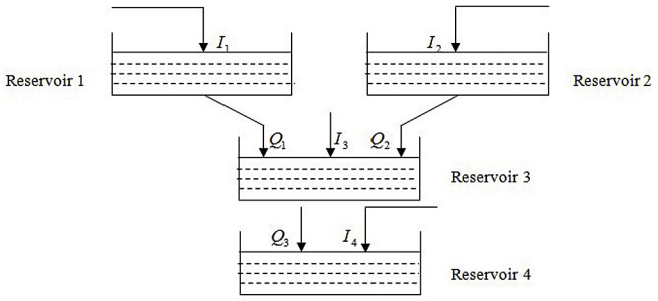

Fig. 9. Hydraulic relationships among the four hydro-plants.

proposed method and other alternatives are taken in this test system. The parameter settings are presented as follows: The population size is 100, the size of archive set is 30, evolutionary generation is 2000, the initial scaling parameter η_0 is set to 0.8, the total permitted accuracy is set to 0.1, coarse adjustment number is 15, fine tuning number is 10, the permitted water balance and output violation is 0.01.

30 non-dominated schemes are produced by the proposed GD-MOCDE in comparison to MODE [13], which can be seen in Fig. 10. It shows that the Pareto optimal schemes by GD-MOCDE dominates that of MODE, and also reveals that GD-MOCDE converges better than MODE. The obtained 30 non-dominated scheduling results are listed in Table 10.

Since few literature take nonlinear transmission loss into consideration, we take comparison with those obtained results without considering transmission loss, which are listed in Table 11. According to obtained results in Table 10, minimum fuel cost by GD-MOCDE is 41853$, which is smaller than ELS result of Refs. [42,13], and minimum emission rate is 17013lb, which is also relative low in comparison to those references. Here, Scheme (15) is considered as compromise scheme with 43225$ and 17422lb, it can be obtained that fuel cost can be better than that in Ref. [42], and has lower emission rate while higher fuel cost than that in Ref. [13], 30 non-dominated schemes are generated in 1011s with each Scheme 37.3s, which is smaller than those methods in Refs. [42,13].

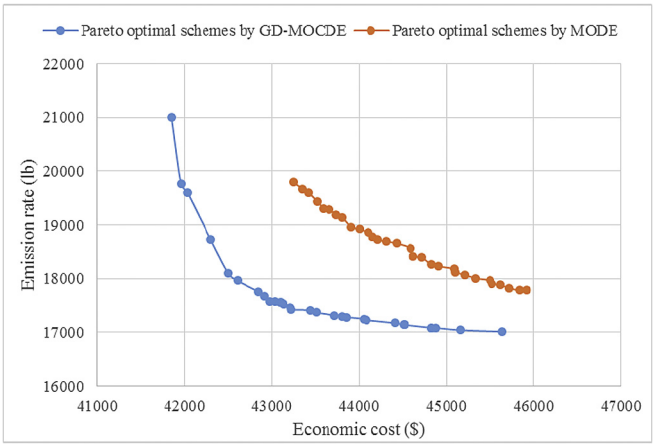

Fig. 10. The comparison between obtained Pareto optimal solutions by GD-MOCDE and MODE for test system 4.

For verifying the viability of obtained optimal schemes, compromise scheme is presented to take further analysis. The water discharge, hydro power output, thermal power output and transmission loss are listed in Table 12, the feasibility of each constraint limit can be checked, and transmission loss can't exceed 1% of system load at each time period.

The storage process of each hydro plant is presented in Fig. 11, it can be seen that hydro plant 3 and hydro plant 4, which are on the downstream and have larger storage ability, have obvious high storage than hydro plant 1and hydro plant 2, then hydro resource can be made full use, more power output can be bear by hydro power to reduce the economic cost and emission volume caused by thermal power.

According to those obtained results by GD-MOCDE on SHOSEE problem, all constraint limits can be properly satisfied, GD-MOCDE can generate a set of non-dominated schemes at relative high efficiency, it can be revealed that GD-MOCDE has great convergence ability and can implement on SHOSEE problem well combing with some constraint-handling techniques.

6.5. Test system 5: hydro-thermal-wind- photovoltaic optimal scheduling

On the basis of hydrothermal system in test system 4, two wind farms and one photovoltaic field are added, and data details are shown in test system 3. In this test system, hydrothermal system represents traditional stable energy resource, wind power and photovoltaic power represent typical intermittent energy resource. The main target of this test system is to minimize the thermal cost and emission volume by properly assigning power output of each power generator under power generation uncertainty caused by intermittent energy resource. For properly tackling with wind power uncertainty, confidence interval is taken to describe the wind power generation process, and probability constraint is handled by the methods presented in Sections 4.3.1 and 4.3.2. The parameter settings are shown as the same as test system 3 and test system 4.

The obtained Pareto front is shown in Fig. 12, 40 non-dominated schemes are produced by GD-MOCDE and MODE, which are shown in Table 13. It can be seen that obtained Pareto front by GD-MOCDE has wider diversity distribution and better convergence efficiency than that by MODE, and the minimum fuel cost and emission volume by GD-MOCDE is smaller than that by MODE. In comparison to hydrothermal optimal scheduling, fuel cost and emission volume of hybrid energy operation decrease sharply especially emission rate after wind farms and photovoltaic field is taken into consideration, which also presents the necessity for integration of renewable energy resources.

The scheme (21) is taken as the compromise scheme for further analysis operation process, its output process of each power generator is shown in Fig. 13. It can be clearly seen that hydro plant #4 provides most output in the hydropower system, which

Table 10
The comparison of non-dominated scheduling results between GD-MOCDE and MODE for test system 4.

Scheme	GD-MOCDE		MODE		Scheme	GD-MOCDE		MODE	
	Thermalcost($)	Emissioncost (lb)	Thermalcost($)	Emissioncost(lb)		Thermalcost($)	Emissioncost(lb)	Thermalcost($)	Emissioncost(lb)
1	41853	20999	43249	19794	16	43446	17414	44589	18567
2	41960	19772	43351	19674	17	43508	17371	44616	18411
3	42035	19598	43422	19598	18	43721	17318	44715	18399
4	42302	18721	43523	19437	19	43806	17290	44827	18264
5	42497	18109	43591	19310	20	43853	17283	44904	18231
6	42604	17964	43659	19282	21	44052	17252	45092	18182
7	42847	17758	43742	19196	22	44086	17229	45108	18123
8	42913	17666	43813	19133	23	44414	17173	45217	18070
9	42972	17581	43911	18963	24	44507	17142	45337	18009
10	43039	17579	44003	18918	25	44525	17140	45498	17967
11	43096	17560	44104	18855	26	44826	17085	45523	17912
12	43105	17558	44156	18775	27	44833	17084	45619	17883
13	43135	17530	44211	18725	28	44880	17083	45717	17827
14	43210	17452	44313	18693	29	45166	17042	45836	17782
15	43225	17422	44434	18654	30	45638	17013	45922	17782

Table 11
Scheduling results in Refs. [13,42].

Objective	Ref. [42] without transmission loss			Ref. [13]		
	ELS	EES	CEES	ELS	EES	SHOSEE
Fuel cost($)	43,500	51,449	44,914	42167	45264	43165
Emission(lb)	21,092	18,257	19,615	19981	16713	17464
Comp. time(s)	72.96	72.74	74.97	–	–	1092 (30 schemes)

can make most full use of hydropower from upstream water discharge. After checking the constraint limits of each power generator, it also can be found that output limits of each power generator and system load balance can be properly satisfied while considering transmission loss effects, which are listed in Table 14. The transmission loss can not exceed 4% of system load at each time interval, which also reveals that transmission loss is properly controlled.

Since hydropower generation mainly depends on the storage and water discharge of each power plant, further analysis is taken on the storage process and water discharge process, which are shown in Figs. 14 and 15. It can be seen that water discharge and storage process are similar with that without considering wind farms and photovoltaic field in shape, which reveals that wind power and photovoltaic power can merely affect the output value of hydro plant, but cannot affect the optimal operation measurement of hydro plant under system load balance constraint, those intermittent energy resources can merely bear the output burden of the whole operation system, the output measurement of each power generator doesn't relate to other energy resources, it only relates to its inner optimal scheduling measurement.

According to above results on the hydro-thermal-wind-photovoltaic power system, the proposed GD-MOCDE can solve SHOSEE-IIER problem well and can produce a set of non-dominated optimal schemes for decision-makers in the hybrid energy system. Simultaneously, it can be found that integration of wind power and photovoltaic can decrease the fuel cost and emission rate sharply, but it can't affect the operation measurement of each power

Table 12
The details of compromise schedule result by GD-MOCDE for test system 4.

Hours	Water discharge($10^{4*}m^3/s$)				Hydro power(MW)				Thermal power(MW)			P_L(MW)	Load(MW)
	Q_1	Q_2	Q_3	Q_4	P_{h1}	P_{h2}	P_{h3}	P_{h4}	P_{s1}	P_{s2}	P_{s3}		
1	9.754	6.068	22.141	6	84.845	49.48	34.664	131.88	175	134.706	143.363	3.938	750
2	7.066	6	23.633	6	68.958	50.127	20.884	129.027	172.105	207.008	136.54	4.649	780
3	7.41	6	23.071	6	71.866	51.258	18.289	125.744	174.54	124.888	137.143	3.728	700
4	8.14	6.01	19.323	6	76.803	52.969	34.377	121.625	103.889	209.776	53.07	2.509	650
5	7.382	6	18.232	6	71.527	54.46	37.023	115.822	128.891	124.949	140.367	3.039	670
6	6.524	6.07	18.025	6	64.995	55.971	37.041	130.943	173.253	203.412	139.048	4.663	800
7	9.454	8.025	19.341	7.125	83.612	69.462	31.881	160.994	174.959	209.686	225.802	6.396	950
8	8.828	6.837	17.96	11.844	79.793	60.788	36.124	230.947	174.914	209.817	223.976	6.359	1010
9	9.754	9.084	18.033	18.232	84.642	74.551	34.431	294.563	175	209.633	223.53	6.35	1090
10	9.775	8.79	17.175	18.025	84.833	72.342	36.721	293.098	174.935	209.706	214.526	6.161	1080
11	10.615	8.263	16.826	19.341	89.01	69.434	38.067	301.966	174.846	209.807	223.212	6.342	1100
12	7.459	6.656	18.977	17.96	72.232	59.569	30.683	292.63	175	209.74	318.799	8.653	1150
13	10.108	10.518	17.559	18.243	88.151	82.379	36.843	294.644	175	210.445	229.018	6.48	1110
14	8.905	7.445	19.699	17.127	82.198	64.181	30.826	286.236	175	126.02	271.757	6.218	1030
15	8.841	9.298	17.888	17.03	82.647	75.831	37.69	285.527	174.973	209.517	148.751	4.936	1010
16	6.238	6.069	17.831	18.611	64.955	55.471	38.626	296.821	174.474	209.699	226.355	6.401	1060
17	8.105	9.111	15.843	17.649	79.333	75.712	45.514	290.371	174.955	209.552	180.048	5.485	1050
18	8.375	10.849	15.593	19.703	81.257	83.038	46.881	304.124	175	209.823	226.286	6.409	1120
19	9.452	12.117	14.531	20	87.619	85.093	49.279	305.904	174.981	209.673	162.628	5.177	1070
20	9.51	12.314	14.925	20	87.378	82.41	48.92	303.735	175	209.642	147.838	4.923	1050
21	6.618	10.806	12.342	19.714	67.68	73.809	51.923	299.792	174.439	124.969	120.896	3.508	910
22	6.109	10.359	12.857	19.898	63.701	70.643	54.53	296.801	112.025	124.914	140.187	2.801	860
23	5.302	11.637	13.365	20	57.091	74.801	56.988	292.725	107.165	124.92	139.032	2.722	850
24	5.275	7.675	13.881	16.905	57.246	53.271	58.215	266.859	106.725	124.357	135.997	2.67	800

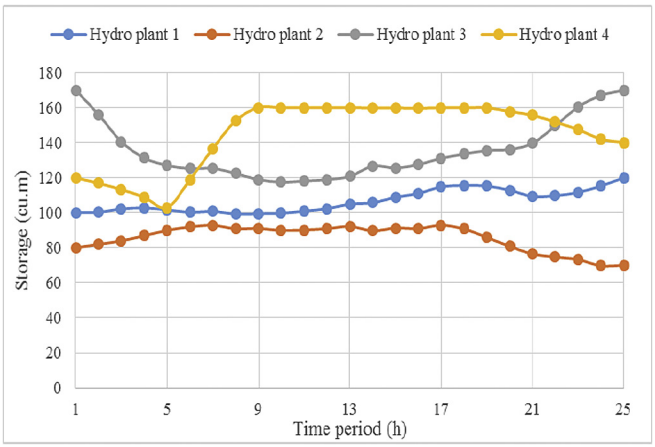

Fig. 11. The storage process of four hydro plants in compromise scheme.

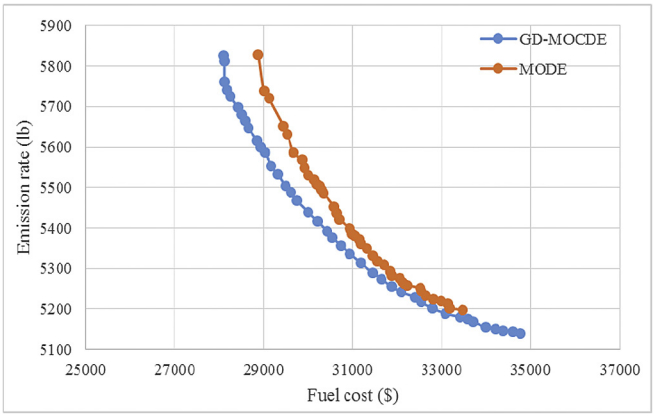

Fig. 12. The obtained Pareto front by GD-MOCDE and MODE for test system 5.

generator, which also reveals that each energy resource can be considered as an independent system, and operation rule merely depends on its own inner characteristics, and we should know more about optimal scheduling rule of each energy resource.

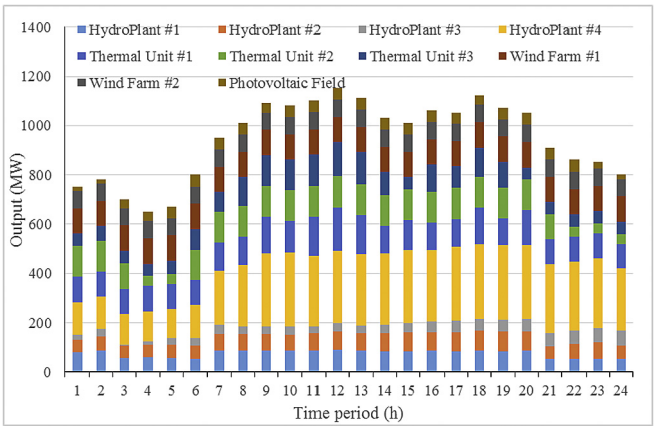

Fig. 13. The output process of hydro-thermal-wind-photovoltaic power in compromise scheme.

7. Conclusion

This study extends hydrothermal optimal scheduling model into optimal scheduling of hybrid energy with integrating wind farms and photovoltaic fields. The hybrid energy system consists of hydro plants, thermal units, wind farms and photovoltaic fields, which makes hybrid energy system difficult to solve economic emission optimal scheduling of hybrid energy system due to its complexity, stochastic and constraint-coupled characteristics. In order to properly solve SHOSEE-IIER problem, this paper proposes a gradient decent based multi-objective cultural differential evolution combining with several constraint-handling techniques. For improving the optimization efficiency, the proposed GD-MOCDE integrates gradient decent operator into cultural differential evolution, which can provide rapid search direction for population evolution and enhance the search ability for seeking optimal solution. Furthermore, several constraint handling techniques are utilized to tackle with probability constraint, water volume balance constraint and system load balance constraint, probability constraint is converted into deterministic constraint, heuristic constraint handling technique is used to deal with water volume water balance and system load balance constraint. Furthermore,

Table 13
The comparison of non-dominated scheduling results between GD-MOCDE and MODE for test system 5.

Scheme	GD-MOCDE		MODE		Scheme	GD-MOCDE		MODE	
	Thermalcost($)	Emissioncost (lb)	Thermalcost($)	Emissioncost(lb)		Thermalcost($)	Emissioncost(lb)	Thermalcost($)	Emissioncost(lb)
1	28107	5825	28884	5828	21	30551	5376	31136	5371
2	28117	5813	29003	5739	22	30734	5357	31174	5360
3	28123	5762	29121	5721	23	30938	5337	31312	5349
4	28178	5741	29445	5652	24	31186	5313	31446	5331
5	28254	5726	29536	5631	25	31448	5290	31549	5319
6	28423	5698	29679	5586	26	31657	5274	31705	5309
7	28498	5681	29871	5568	27	31877	5255	31833	5294
8	28578	5664	29922	5549	28	32096	5242	31882	5283
9	28670	5646	29995	5530	29	32411	5229	32057	5275
10	28853	5616	30137	5520	30	32534	5218	32114	5266
11	28943	5601	30188	5509	31	32788	5202	32159	5263
12	29032	5587	30254	5504	32	33075	5189	32234	5259
13	29165	5554	30284	5496	33	33415	5180	32512	5251
14	29329	5532	30354	5487	34	33585	5175	32542	5245
15	29488	5504	30585	5453	35	33694	5169	32640	5234
16	29611	5488	30645	5437	36	33986	5155	32805	5224
17	29740	5469	30701	5422	37	34208	5150	32981	5221
18	29992	5440	30927	5399	38	34386	5147	33141	5213
19	30209	5417	30981	5386	39	34588	5144	33177	5203
20	30421	5392	31045	5380	40	34777	5140	33471	5198

Table 14
The transmission loss of hydro-thermal-wind-photovoltaic power system.

Period(h)	1	2	3	4	5	6	7	8	9	10	11	12
Loss (MW)	1.76	1.82	1.615	1.243	1.281	2.023	2.154	2.522	3.135	2.797	3.325	3.757
Period(h)	13	14	15	16	17	18	19	20	21	22	23	24
Loss (MW)	3.349	2.24	1.979	2.403	2.218	3.039	2.343	2.23	1.586	1.248	1.247	1.224

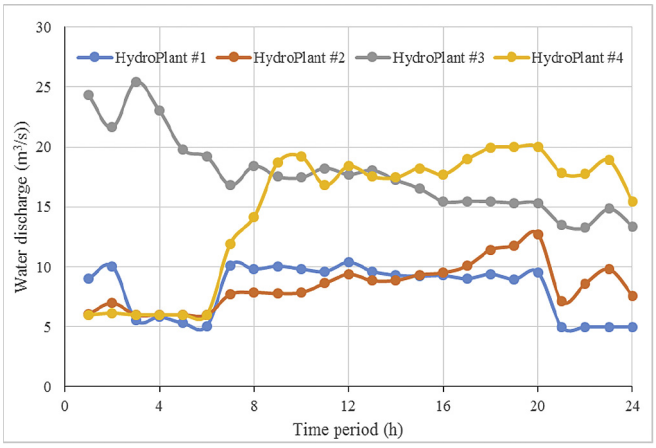

Fig. 14. The water discharge process of four hydro plants in compromise scheme.

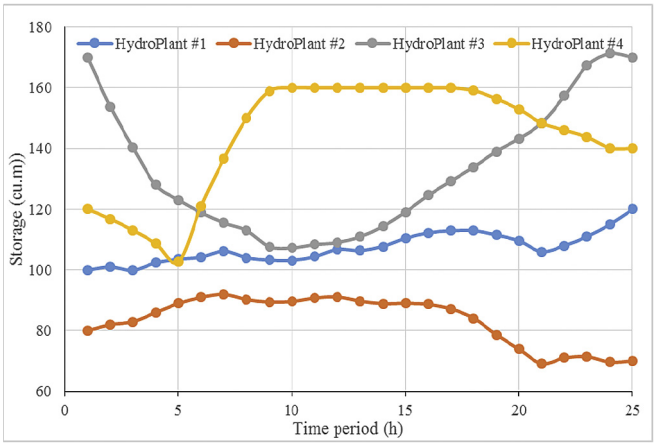

Fig. 15. The storage process of four hydro plants in compromise scheme.

five test systems are utilized to verify the efficiency of the proposed GD-MOCDE, it can be found that integration of wind power and photovoltaic can decrease the fuel cost and emission rate caused by thermal units sharply, and GD-MOCDE can optimize SHOSEE-IIER problem well combined with some constraint-handling techniques.

Acknowledgement

This work is supported by National natural fund (NO.61503199), National natural science key fund (NO.61533010), the Ph. D. Programs Foundation of Ministry of Education of China (NO.20110142110036), Jiangsu Province natural science fund (NO.BK20150853), Jiangsu Province post-doctoral fund (NO.1501042C), Jiangsu Province high school natural science fund (NO.15KJB120009), NUPTSF (NO.NY214206), Open Fund (Grant NO.XJKY14019).

References

[1] Mandal KK, Chakraborty N. Daily combined economic emission scheduling of hydrothermal systems with cascaded reservoirs using self organizing hierarchical particle swarm optimization technique. Expert Syst Appl 2012;39:3438–45.
[2] Gil E, Bustos J, Rudnick H. Short-term hydrothermal generation scheduling model using a genetic algorithm. Power Syst. IEEE Trans 2003;18(4):1256–64.
[3] Senthil Kumar V, Mohan MR. A genetic algorithm solution to the optimal short-term hydrothermal scheduling. Int J Electr Power Energy Syst 2011;33(4):827–35.
[4] Ramirez MO. The short-term hydrothermal coordination via genetic algorithms. Electr Power Comp Syst 2006;34:1–19.
[5] Yuan XYY. A hybrid chaotic genetic algorithm for short-term hydro system scheduling. Math Comput Simul 2002;59(4):319–27.
[6] Suzannah Yin, Wa Wong. Hybrid simulated annealing/genetic algorithm approach to short-term hydro-thermal scheduling with multiple thermal plants. Int J Electr Power Energy Syst 2001;23(7):565–75.
[7] Basu M. An interactive fuzzy satisfying method based on evolutionary programming technique for multiobjective short-term hydrothermal scheduling. Electr Power Syst Res 2004;69(2):277–85.
[8] Ngoc Dieu Vo, Ongsakul Weerakorn. Improved merit order and augmented Lagrange Hopfield network for short term hydrothermal scheduling. Energy Convers Manag 2009;50:3015–23.
[9] Wang Ying, Zhou Jianzhong, Zhou Chao, Wang Yongqiang, Qin Hui, Lu Youlin. An improved self-adaptive PSO technique for short-term hydrothermal scheduling. Expert Syst Appl 2012;39:2288–95.
[10] Amjady Nima, Soleymanpour Hassan Rezai. Daily hydrothermal generation scheduling by a new modified adaptive particle swarm optimization technique. Electr Power Syst Res 2010;80:723–32.
[11] Lu Youlin, Zhou Jianzhong, Qin Hui, Wang Ying, Zhang Yongchuan. An adaptive chaotic differential evolution for the short-term hydrothermal generation scheduling problem. Energy Convers Manag 2010;51:1481–90.
[12] Sivasubramani S, Shanti Swarup K. Hybrid DE–SQP algorithm for non-convex short term hydrothermal scheduling problem. Energy Convers Manag 2011;52:757–61.
[13] Zhang Huifeng, Zhou Jianzhong, Zhang Yongchuan, Lu Youlin, Wang Yongqiang. Culture belief based multi-objective hybrid differential evolutionary algorithm in short term hydrothermal scheduling. Energy Convers Manag 2013;65:173–84.
[14] Qin Hui, Zhou Jianzhong, Lu Youlin, Wang Ying, Zhang Yongchuan. Multi-objective differential evolution with adaptive Cauchy mutation for short-term multi-objective optimal hydro-thermal scheduling. Energy Convers Manag 2010;51:788–94.
[15] Youlin Lu, Jianzhong Zhou, Hui Qin, Qin Hui, Wang Ying, Zhang Yongchuan. A hybrid multi-objective cultural algorithm for short-term environmental/economic hydrothermal scheduling. Energy Convers Manag 2011;52(5):2121–34.
[16] Deb K. Multi-objective optimization using evolutionary algorithms. Chichester (UK): Wiley; 2001.
[17] Kalyanmoy D, Amrit P, Sameer A, Meyarivan T. A fast and elitist multi-objective genetic algorithm: NSGAII. IEEE Trans Evol Comput 2002;6(2):182–97.
[18] Zitzler E, Laumanns M, Thiele L. SPEA2: improving the strength Pareto evolutionary algorithm. Technical report 103, computer engineering and networks laboratory (TIK). Gloriastrasse 35, CH-8092. Zurich, Switzerland: Swiss Federal Institute of Technology (ETH); 2001. Zurich.
[19] Wang Y, Yang Y. Particle swarm with equilibrium strategy of selection for multi-objective optimization. Eur J Oper Res 2010;200(1):187–97.
[20] Tripathi PK, Bandyopadhyay S, Pal SK. Multi-objective particle swarm optimization with time variant inertia and acceleration coefficients. Inf Sci 2007;177(22):5033–49.
[21] Xue F, Sanderson AC, Graves RJ. Pareto-based multi-objective differential evolution. In: Proceedings of the 2003 congress on evolutionary computation (CEC'2003), vol. 2. Canberra (Australia): IEEE Press; 2003. p. 862–9.
[22] Rolic T, Filipic B. DEMO: differential evolution for multi-objective optimization. Lecture Notes Comput Sci. Berlin: Springer; 2005. p. 520–33.
[23] Qian W. And others, adaptive differential evolution algorithm for multi-objective optimization problems. Appl Math Comput 2008;201(1):431–40.
[24] Yuan XH, Tian H, Yuan YB, Huang YH, Ikram RM. An extended NSGA-III for solution multi-objective hydro-thermal-wind scheduling considering wind power cost. Energy Convers Manag 2015;96:568–78.

[25] Salgado CJL, Ano O, Ojeda-Esteybar DM. Energy and reserve co-optimization within the Short Term Hydrothermal Scheduling under uncertainty: a proposed model and decomposition strategy. Electr Power Syst Res 2016;140:539–51.
[26] Dubey HM, Pandit M, Panigrahi BK. Ant lion optimization for short-term wind integrated hydrothermal power generation scheduling. Int J Electr Power Energy Syst 2016;83:158–74.
[27] Cai J, Ma X. A multi-objective chaotic particle swarm optimization for environmental/economic dispatch. Energy Convers Manage 2009;50(5):1105–13.
[28] Basu M. Particle swarm optimization based goal-attainment method for dynamic economic emission dispatch. Electr Power Comp Syst 2006;34:1015–25.
[29] Storn R, Price K. Differential evolution-a simple and efficient adaptive scheme for global optimization over continuous spaces. Berkeley: ICSI, University of California; 1995.
[30] Reynolds RG. An introduction to cultural algorithms. In: Sebalk AV, Fogel River Edge NJ, editors. Proceedings of the 3rd annual conference on evolution programming. World Scientific Publishing; 1994. p. 131–6.
[31] Saleem SM. Knowledge-based solution to dynamic optimization problems using cultural algorithms. PhD thesis. Detroit, Michigan: Wayne State University; 2001.
[32] Yuenyong S, Nishihara A. A hybrid gradient-based and differential evolution algorithm for infinite impulse response adaptive filtering. Int J Adapt Control Singnal Process 2014;10(28):1054–64.
[33] Bello Cruz JY, Lucambio Perez LR, Melo JG. Convergence of the projected gradient method for quasiconvex multiobjective optimization. Nonlinear Analysis Theory Methods Appl 2011;16(74):5268–73.
[34] Jean-Antoine Desideri. Multiple-gradient descent algorithm (MGDA) for multiobjective optimization. Comptes Rendus Math 2012;350(5–6):313–8.
[35] Yu Gang, Chai Tianyou, Luo Xiaochuan. Multiobjective production planning optimization using hybrid evolutionary algorithms for mineral processing. IEEE Trans Evol Comput 2011;15(4):487–514.
[36] Gelbard Roy, Carmeli Abraham, Bittmann Ran M, Ronen Simcha. Cluster analysis using multi-algorithm voting in cross-cultural studies. Expert Syst Appl 2009;36(7):10438–46.
[37] Immanuel A, Thanushkodi K. A new particle swarm optimization solution to nonconvex economic dispatch problems. IEEE Trans Power Syst 2007;22(1):42–50.
[38] Zhang Haifeng, Gao Feng, Wu Jiang, Liu Kun. A dynamic economic dispatching model for power grid containing wind power generation system. Power Syst Technol 2013;37(5):1298–303.
[39] Karaki SH, Chedid RB, Ramadan R. Probabilistic performance assessment of autonomous solar-wind conversion system. IEEE Trans Energy Convers 1999;14(3):766–72.
[40] Qu BY, Liang JJ, Zhu YS, Wang ZY, Suganthan PN. Economic emission dispatch problems with stochastic wind power using summation based multi-objective evolutionary algorithm. Inf Sci 2016;351:48–66.
[41] Lu Youlin, Zhou Jianzhong, Qin Hui, Qin Hui, Wang Ying, Zhang Yongchuan. A hybrid multi-objective cultural algorithm for short-term environmental/economic hydrothermal scheduling. Energy Convers Manage 2011;52(5):2121–34.
[42] Kalyanmoy D, Amrit P, Sameer A, Meyarivan T. A fast and elitist multiobjective genetic algorithm: NSGAII. IEEE Trans Evol Comput 2002;6(2):182–97.
[43] Pandit N, Tripathi A, Tapaswi S, Pandit M. An improved bacterial foraging algorithm for combined static/dynamic environmental economic dispatch. Appl Soft Comput 2012;12(11):3500–13.
[44] Jiang XW, Zhou JZ, Wang H, Zhang YC. Dynamic environmental economic dispatch using multiobjective differential evolution algorithm with expanded double selection and adaptive random restart. Int J Electr Power Energy Syst 2013;49:399–407.
[45] Aghaei J, Niknam T, Azizipanah-Abarghooee R, Arroyo JM. Scenario-based dynamic economic emission dispatch considering load and wind power uncertainties. Int J Electr Power Power Syst 2013;47:351–67.